

STATISTICAL STRAY ENERGY MONITOR

By

JIMMIE DICK BURSON

Bachelor of Science

Oklahoma State University

Stillwater, Oklahoma

1959

Submitted to the faculty of the Graduate College of  
the Oklahoma State University  
in partial fulfillment of the requirements  
for the degree of  
MASTER OF SCIENCE  
May, 1967

T. Shesha  
1967  
B9772nd  
copy 2

OKLAHOMA  
STATE UNIVERSITY  
LIBRARY  
JAN 9 1968

STATISTICAL STRAY ENERGY MONITOR

Thesis Approved:

Paul A. McCollum  
Thesis Adviser

Harold F. Frazier

N. D. Durham  
Dean of the Graduate College

658373

## PREFACE

Stray electromagnetic energy is present everywhere in the environment where we live and work. It can be both useful and detrimental. The presence of this energy is not readily determined by the human senses and must be measured by other methods. Although a number of instruments are available to monitor stray energy automatically, they are generally complicated and bulky. It is desirable to have an instrument that is small, light, and operates unattended, and that will monitor this stray energy automatically and process it in a statistical manner.

Before such an instrument can be developed, it is desirable that the designer should demonstrate the feasibility of the concept. The feasibility may be proven analytically; however, a demonstration in the laboratory is more acceptable. The purpose of this investigation then is to experimentally demonstrate the design feasibility of a statistical stray energy monitor (SSEM).

A unique sensor-detector was designed specifically for use in the monitoring of stray energy that may be present in electroexplosive subsystems on aircraft. A major difficulty was encountered in the effort to obtain high common mode rejection for the detector circuit which must operate at high impedances and wide bandwidths. The selection of a voltage doubler detection method followed by a differential-input source follower overcame this problem.

Indebtedness is acknowledged to Dr. W. L. Hughes, Professor Paul A. McCollum, and Dr. H. T. Fristoe for their valuable guidance, and their assistance in the procurement of much of the solid-state modules and components, and to the following for their contributions to this investigation: Gene Morgan, Dr. R. D. Strattan, Don Sandkuhl, Mary Horrall and Dorothy Christie of North American Aviation; Claude Austin, Air Force Avionics Laboratory; Robert Parker, Sandia Corporation; Clyde Lumpkin, Century Electronics; Wendell McCracken, Collins Radio Company; and Carl Geller, Motorola Semiconductor Division.

I am grateful to the Oklahoma State University Electrical Engineering College which provides "after hours" courses and laboratory facilities for those of us who pursue degrees while fully employed. I especially wish to thank both Dr. Hughes and Professor McCollum for their time spent in excess of their normal duties. I wish to express my gratitude to Donna, my wife, who understood, believed-in, encouraged, and upheld me throughout the pursuit of this degree.

## TABLE OF CONTENTS

Chapter		Page
I.	THE PROBLEM . . . . .	1
	Statement of the Problem . . . . .	1
	Practical Limitations of a Feasibility Demonstration . . . . .	2
	Design Philosophy and Concept . . . . .	3
II.	REVIEW OF THE LITERATURE . . . . .	7
	Historical Background . . . . .	7
	Sensor Availability . . . . .	8
	Characteristics of Existing Instrumentation . . . . .	9
	Summary of the Literature . . . . .	13
III.	DESIGN OF INSTRUMENT . . . . .	15
	Analysis and Design . . . . .	15
	System Operation . . . . .	30
	Fabrication of Breadboard . . . . .	38
	Checkout and Calibration . . . . .	47
IV.	EXPERIMENTAL TEST DATA . . . . .	50
	Treatment of Test Data . . . . .	50
	Correlation With Design Analysis . . . . .	51
V.	RESULTS AND SUMMARY . . . . .	55
	Discussion of Test Results . . . . .	55
	Summary and Conclusions . . . . .	55
	BIBLIOGRAPHY . . . . .	58

## LIST OF TABLES

Table		Page
I.	Material List for Breadboard Model . . . . .	6
II.	List of Test Equipment . . . . .	49
III.	Test Data Obtained During Sampling Period . . . . .	52

## LIST OF FIGURES

Figure		Page
1.	Statistical Stray Energy Monitor (SSEM) . Block Diagram . . . . .	4
2.	Typical Output Data Distribution . . . . .	6
3A.	Voltage Doubler Detector Circuit . . . . .	16
3B.	Equivalent Circuit for Common Mode Calculations . . . . .	16
4A.	Differential Input Integrated Circuit Amplifier . . . . .	21
4B.	Peak Detector and Impedance Transforming Circuit . . . . .	21
5.	Signal Conditioner Block Diagram . . . . .	31
6.	Analog-to-Digital Converter (ADC) Block Diagram . . . . .	32
7.	Data Processor Block Diagram . . . . .	33
8.	Timing Diagram (SSEM) . . . . .	34
9A.	Power Switching Circuit . . . . .	37
9B.	Sensor-Detector Schematic Diagram . . . . .	37
10.	8421 Up-Counter Connection Diagram . . . . .	40
11.	Threshold-Count Logic Connections . . . . .	42
12.	Timing Circuit Connections . . . . .	43
13.	Plot of Actual Data Distribution Obtained During Test Monitoring of Stray Energy . . . . .	53



## CHAPTER I

### THE PROBLEM

There is a need for an instrument that will measure stray electromagnetic energy and will operate unattended over a wide range of operating conditions. Furthermore, the instrument must monitor continuously without interfering with the system it is monitoring. One specific application requiring such a device is the gathering of data describing the electromagnetic environment to which an electroexplosive device (EED) is subjected. These EED's are located in various physical locations aboard military aircraft. The wires connecting the electrical firing source to the EED may act as antennas and pick up stray electromagnetic energy. This energy is impressed across the EED and will in fact cause a premature initiation of the EED if certain energy levels are exceeded. If a monitor is installed aboard an aircraft at each EED location (or selected EED locations), the data collected describe the electromagnetic energy environment to which the EED's have been subjected.

#### Statement of the Problem

Presently, there is no satisfactory means for adequately measuring the stray energy in a statistical manner while the EED system is performing its intended mission. An extremely small device is needed which can process the data in

some manner and store only the essential characteristics of the data. Meaningful data are needed from which to assess the probability of a hazard due to stray electromagnetic energy prematurely initiating the EED. Some form of a statistical distribution of the magnitude of the signal at the EED is necessary to accomplish this task.

Since the primary purpose is to determine whether or not a potential problem exists, the monitor must operate continuously over relatively long periods of time. The data obtained in distributional form should facilitate a mathematical probability analysis of the electromagnetic hazard encountered by an EED in its normal service or environment.

Such a device might be termed a Statistical Stray Energy Monitor (SSEM) and could consist of a sensor-detector followed by a digital data processor and storage device which would store and hold a histogram of the data coming from the detector.

#### Practical Limitations of a Feasibility Demonstration

The complete development of such a device would entail a much larger effort than can be expected from a master's thesis research project. However, this paper describes the development and operation of a breadboard model in sufficient detail to demonstrate the feasibility of the device. It was felt unnecessary to fully implement the desired capacity of the storage register or the multitude of discrete amplitude levels to be detected. For the most part, standard laboratory-type logic modules were available which satisfactorily duplicated the desired electrical functions of the monitor.

The environment to which the model is normally subjected was simulated by signal generators in the laboratory. The operation of the monitor was observed for a limited number of samples at several levels of amplitude. This corresponds to the demonstration of a single channel receiver to determine the feasibility of a multi-channel device. Each function of the monitor was demonstrated by newly designed and built circuits where possible and by laboratory equipment when actual circuitry was already developed and available. These limitations do not invalidate the feasibility of the concept.

### Design Philosophy and Concept

The statistical stray energy monitor provides a means for gathering, processing and storing data derived from stray electromagnetic energy that has been coupled onto the firing-circuit wiring of pyrotechnic initiators (EED's). The collected data were then used in a statistical analysis to determine the arithmetic mean ( $\bar{x}$ ) and the standard deviation ( $\sigma$ ) of the stray energy which has been coupled onto the circuit under consideration.

The actual quantity being measured by the monitor was peak voltage, since a peak-detecting crystal diode detector was utilized.

The monitor was designed to gather data efficiently under the constraints of power and size. A block diagram is shown in Figure 1. The concept is a data processor that performs the following operations:

1. Counts the number of data samples gathered during the test period for each of several levels.

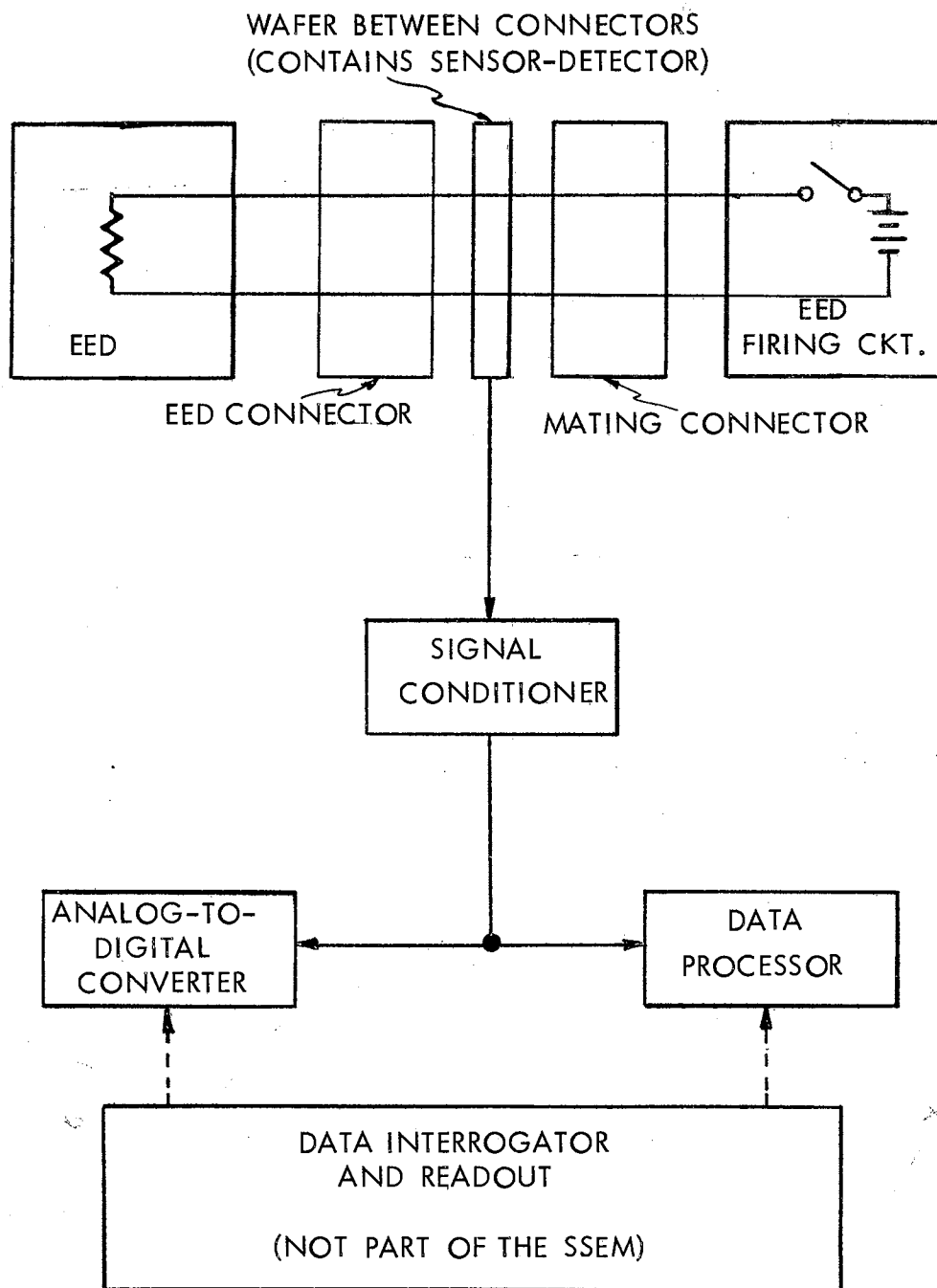


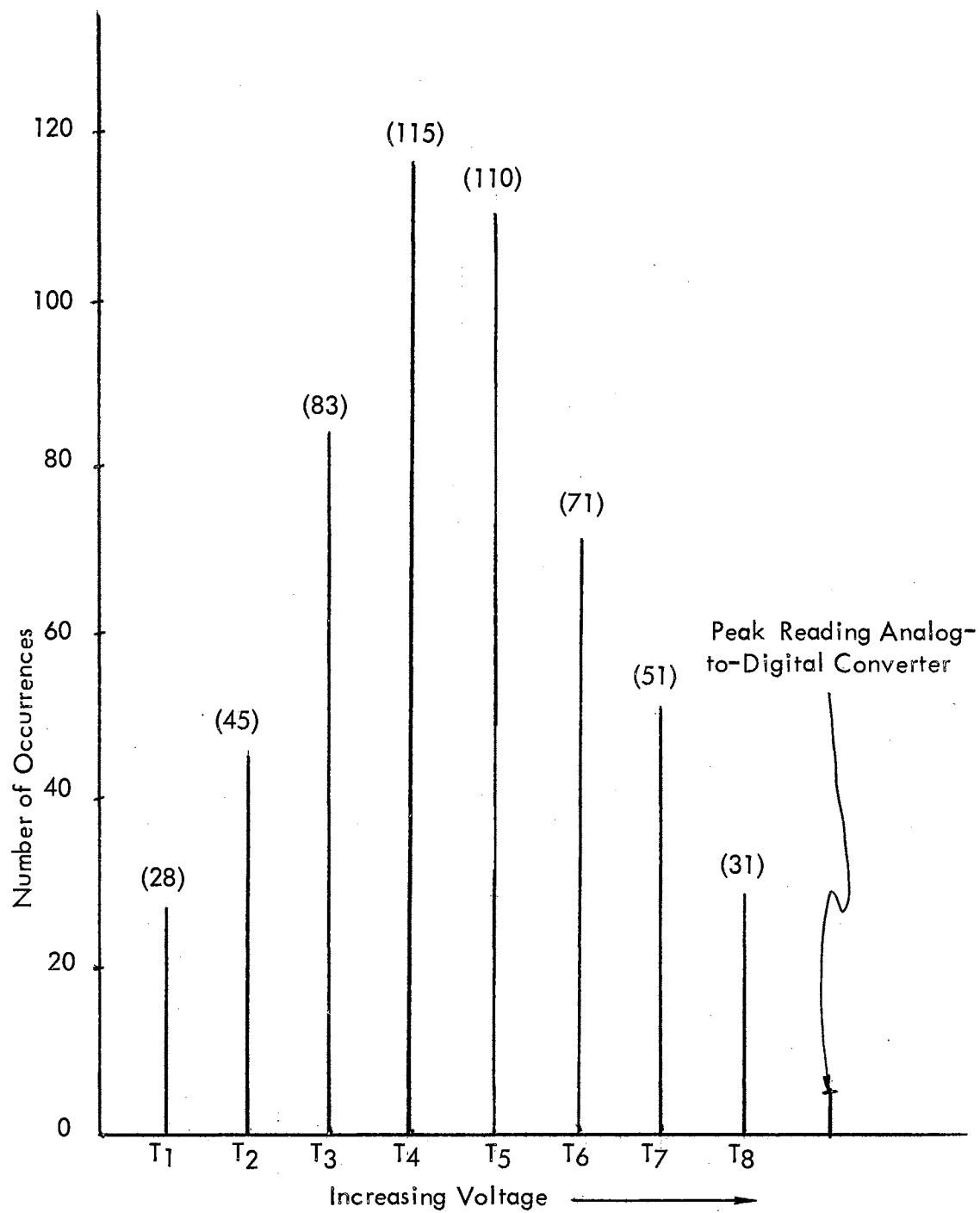
Figure 1. Statistical Stray Energy Monitor (SSEM)  
Block Diagram

2. Digitizes the largest value data sample encountered during the test period.
3. Stores the total number of data samples encountered (sum of all counters).

Over a period of time, a typical data distribution might look like that in Figure 2. The coordinates of the graph are Number of Occurrences versus Voltage. The numbers in parenthesis are a count of the data samples which occurred at each threshold level of voltage. A statistical analysis of the data distribution could then be performed using this graph. The largest value sample encountered during the test period is measured by the peak reading Analog-to-Digital Converter (ADC).

The breadboard model used both discrete components and integrated circuits. If the SSEM were placed into production, the final production design of the detector section would incorporate integrated circuits so that it could be physically placed between the pins of the pyrotechnic connector. A small, thin wafer would be used to mount the detector. The wafer would be placed between the connector and the pyrotechnic device.

The SSEM in service would be shielded from EM radiation and would be placed near the pyrotechnic to reduce inductive coupling in the detector wiring. It would also be battery powered to eliminate conducted interference as much as possible. These design constraints apply only to the final production design and not to the actual breadboard model which is the subject of this paper.



Note: T<sub>1</sub>, ...T<sub>8</sub> = Detector Thresholds

Figure 2. Typical Output Data Distribution

## CHAPTER II

### REVIEW OF THE LITERATURE

#### Historical Background

Many monitoring systems have been studied by those agencies concerned with the problem of electromagnetic hazards to EED's and several of these have been implemented. However, only a small number of these systems have been thoroughly analyzed and very few of those analyzed have shown sufficient promise to warrant a full development and evaluation program. Most of this research effort has been devoted to sensor development. Design of the compatible peripheral equipment has been determined by the requirements established by the sensor characteristics. Sensor design has been plagued by more problems than any other single component in the monitoring system. This is attributed to the stringent requirements on sensitivity, frequency response, and accuracy; these requirements are complicated by the necessity for locating the sensing element in the immediate vicinity of the EED firing element. This constraint establishes conditions conducive to a change in the electrical characteristics of the EED, a condition which must be avoided by careful and selective sensor design.

The results of the literature survey conducted by the writer show that monitor systems have been divided into three general classes of systems:

(1) systems which have been developed and are being used by various laboratories and agencies, (2) systems which have been fairly well analyzed or developed but are not widely used and, (3) proposed methods of monitoring.

### Sensor Availability

A wide range of sensors are available for use in monitoring stray electromagnetic energy; however, the literature survey was limited to those useful for in-circuit monitoring of electro-explosive subsystems.

The monitoring of the electromagnetic energy has been accomplished by the direct measurement of electrical power, voltage or current. Since in many instances the electromagnetic energy is transformed into other forms of energy, sensors for measuring thermal energy, light energy, gas pressure and long wavelength radiation were investigated.

Various means of detecting these forms of energy were found to be available. Among those types of sensors applicable to the problem are thermocouples, thermistors, infrared devices, pyroelectric devices, Hall-effect detectors, crystal-diode detectors, Golay cells, temperature-sensitive paint, and other more complex instrumentation. After a cursory examination of the characteristics of these devices, a few were selected for more detailed investigation. The following sensors appeared to offer the most advantages for this design concept: (1) thermocouple, (2) thermistor, (3) crystal diode detectors, and (4) infrared detectors. These devices have all been developed and are available commercially. Their small size and low power requirements make them desirable for the application. Electrical current



sensing devices were ruled out due to the excessive loading on the circuit to be measured.

### Characteristics of Existing Instrumentation

Thermocouples - These sensors have received broader application in EED stray energy monitoring than any other type of detector. The electromagnetic energy is transformed into thermal energy which is then detected by the thermocouple. Although thermocouples have some objectional features when used as sensors to measure power dissipated in EED's, the advantages offered by the wide choice of applications sometimes outweigh their limitations. Thermocouples have undergone extensive development and improvement programs aimed at eliminating or reducing their undesirable features. They are now in use by almost every laboratory that is involved in electromagnetic energy monitoring as related to EED's. Recent research programs are striving for further refinement which will increase the sensitivity, decrease the response time, and improve the frequency response of the total package (1). Other research is directed toward quantitatively isolating those factors which are major contributors to thermocouple errors.

Early thermocouple models had relatively massive elements and were connected to the firing element of heat-initiated EED's. This direct connection affected the impedance of the EED at higher frequencies and loaded the EED firing circuit. An improvement to this device was the hydrogen-filled glass envelope containing the thermocouple junction. Denver Research Institute performed studies on a vacuum-deposited thermocouple consisting of minute

layers of dissimilar metals deposited on a dielectric substrate (2). The thin layers permitted a small-mass junction producing a decrease in the thermal time constant. The device functioned on radiated heat and was electrically isolated from the EED element. Many other attempts have been made to improve the vacuum-deposited thermocouple but have met with only a minimum amount of success. This device still suffers from lack of sensitivity (only 4 db below one milliwatt of electrical power), and it also affects the high-frequency characteristics of the EED itself.

Thermistor Detectors - Thermistors are heat-sensing devices which have a much better sensitivity than existing thermocouples. Sensitivities on the order of 15 db below one milliwatt of electrical power have been achieved under laboratory conditions. These are usually operated in a simple balanced bridge system. Unbalance of the bridge due to ambient heat changes is their most serious limitation. They are therefore not suited for unattended operation that encounters a changing temperature environment. They also suffer in response time characteristics. Thermistor detectors are frequently used in ground tests and laboratory operations for calibration of other systems.

Infrared Detectors - The principal characteristics which make these devices desirable are the short response time and the ability to function on radiated energy. Depending somewhat on the associated electronic circuitry, the time response ranges between that of the thermocouple and the crystal diode detector. This range is considered adequate for monitoring of laboratory testing under CW conditions but is not applicable for extremely short pulses of

a few microseconds duration.

The sensitivity of infrared systems is dependent on both the photocell noise and the bandpass of the overall system. Sensitivities have been achieved on the order of 30 db below one milliwatt of electrical power (3). However, a sensitivity of 20 db below one milliwatt of electrical power is more likely when passband considerations are included. The system has an inherent high photoconductor noise level requiring the use of a mechanical chopper. This becomes a problem when considering the desired miniaturization aspects of the monitor. This limits its application to ground instrumentation and calibration systems and not in-service application to live EED's aboard aircraft (4).

Crystal Diode Detectors - Of the many methods reviewed, the crystal diode detector, which was developed and applied to monitoring electromagnetic energy by the Sandia Corporation, offers the best set of parameters for monitoring of stray energy in EED circuits (5). The detector has good sensitivity, approaching 60 db below one milliwatt of electrical power using biasing techniques, a short response time, and a very low electrical loading effect. The detector may be used without interfering with the normal operation of the EED, thus it is highly suitable for in-service monitoring.

This high level of sensitivity was obtained at a narrow modulation bandwidth of 5 KHz which was not desirable for the wide bandwidth application. However, modulation bandwidths up to 500 KHz have been obtained at a carrier frequency of 10 GHz while still retaining a sensitivity of 35 db below one milliwatt of electrical power. This is considered sufficient sensitivity for the sensor system of the monitor.

The response time of the detector is much better than the other sensors evaluated, a minimum-detectable pulse width on the order of one microsecond is probable. This short response time is highly desirable since it is necessary to monitor random RF transients from sources such as circuit interruptions, lightning strikes, and illumination by high power transmitters. Since wideband operation is desired, the system immediately following the detector was designed for low noise operation in order to enhance the sensitivity of the system.

A diode detector provides excellent electrical isolation due to the high electrical impedance in the backward direction. It is usually high enough to permit placement of the diode detector directly across the EED wiring. The sensing element of the detector operates on a self-powered principle similar to thermocouples. However, the detected signal is small and requires amplification. The sensor diodes are susceptible to destruction by very high power signals but have good stability and can operate for long periods without repeated calibration.

Peripheral Equipment - The most common method of data-conditioning equipment in the past has been simple electronic systems. Some sensors require no signal conditioning and require only hard wire connections to recorders and displays. Recent work with low-power detectors has necessitated the use of amplifiers which instigated more sophistication into the equipment. Also, as more complexity is added, space and weight limitations become restrictive for airborne applications thereby miniaturization becomes necessary.

For in-service applications, completely self-contained systems of small size are required. These needs are best met by integrated circuit techniques. These have the disadvantages of higher power consumption than discrete element design and a trade-off must be made. High density recorders are available and are compatible with rapid data reduction techniques, but their size and power requirements are excessive. Miniaturized, self-contained oscillograph recorders have been designed and one unit has been developed by the Naval Weapons Laboratory (6). The basic disadvantages of the oscillograph are that the frequency response is limited by the chart recording speed and the galvanometers, sensitivity is limited by the galvanometers, and recording time is limited by the chart speed and chart storage capacity.

#### Summary of the Literature

A number of types of detectors were investigated through a review of the literature. Some of these are still under development (7). In addition, several different designs of recording equipment were also investigated. As a result of this survey, it is concluded that the crystal diode detector was the best because of its simplicity, sensitivity, wide frequency coverage, fast response, and small size and weight.

The problem of stray energy monitoring goes beyond the detector. Just as important is the means by which data are recorded or stored. Although several recording and storage devices were studied, the conclusion was reached that most are unsuited because of their size, weight, and power requirements.

Since no extremely small device was discovered that would (1) detect the stray energy, (2) process the data and (3) store the essential characteristics of the data; a device was designed to meet these requirements and its feasibility demonstrated in the laboratory under simulated environment conditions.

## CHAPTER III

### DESIGN OF INSTRUMENT

#### Analysis and Design

Sensor-Detector— The crystal diode detector was selected after consideration of many other types of detectors. Since most EED firing circuits are isolated from ground and use a twisted shielded pair as the firing cable, the detector was designed with a differential input which was isolated from ground. This dictated a bridge-type circuit; however, a full-wave bridge rectifier has a common mode rejection ratio of one. A back-to-back series type peak-detecting circuit has good impedance characteristics but also has poor common mode rejection. A standard voltage doubler circuit overcomes both of these deficiencies. This type of detector has been utilized by Sandia; however, they found that the best characteristics were achieved by reversal of the polarity of one of the diodes.

In reference to Figure 3A, the circuit arrangement is such that the load current flows in one direction through  $R_L$  for each half cycle of input voltage (considering a sine wave input). Since  $C_1$  and  $C_2$  are so much larger than the other capacitors, the effect of  $C_3$ ,  $C_4$ ,  $C_5$ , and  $C_6$  are negligible for the normal output  $e_o$ . Since the diode current flows through  $R_L$ , the output voltage is:

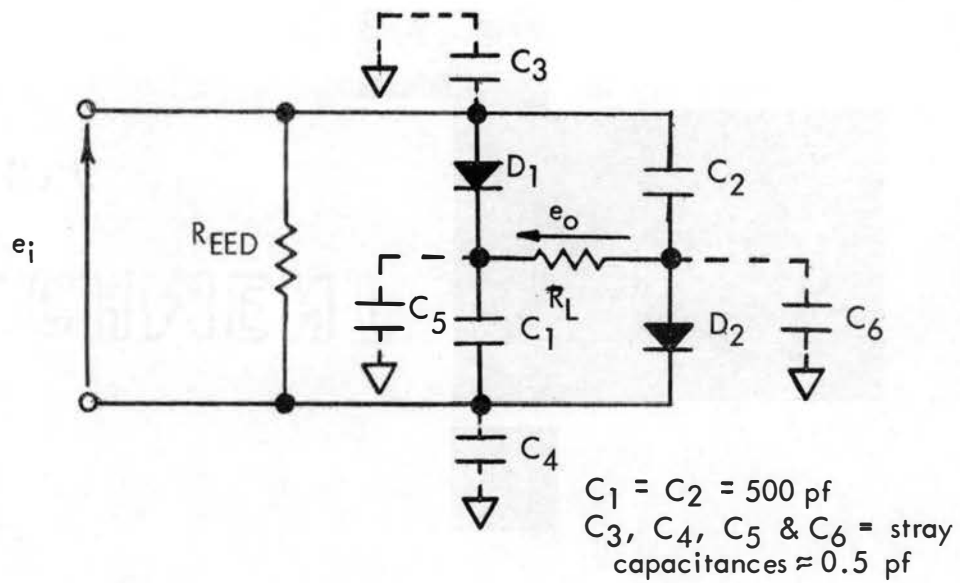
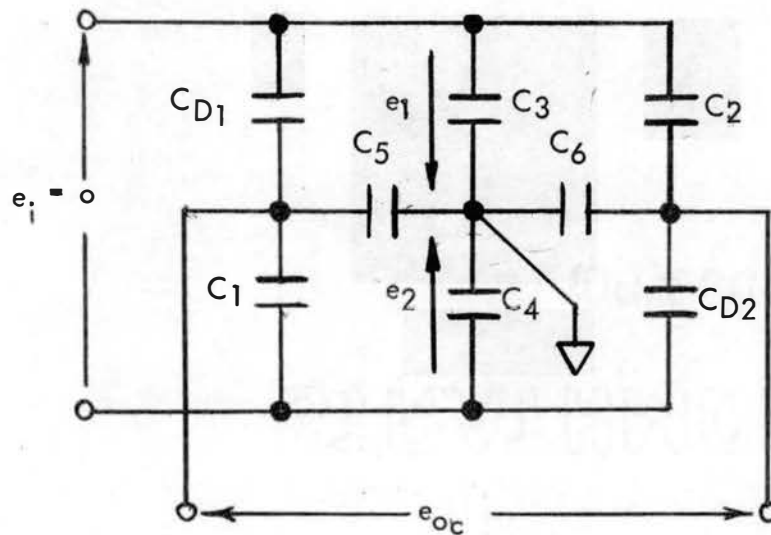


Figure 3A. Voltage Doubler Detector Circuit



Common mode rejection maximum when  $e_1 = e_2$

Figure 3B. Equivalent Circuit for Common Mode Calculations



$$e_o = k(e_{in})^2.$$

However, since the voltages add, to maintain the same load on each diode as in the previous circuit (diode not reversed), the load resistance was doubled. Since the diode detectors are current generators (for small signal detection), doubling the load resistance doubles the output voltage; therefore the equation becomes:

$$e_o = 2K(e_{in})^2.$$

This indicates the "voltage doubling" action of the circuit. Actually, the circuit arrangement provides full wave detection since capacitors  $C_1$  and  $C_2$  are charged on the positive half cycle and then discharged on the negative half cycle to provide current flow through  $R_L$  during the entire cycle.

An analysis was made of the common mode rejection characteristics using the equivalent circuit shown in Figure 3B. For common mode calculations,  $e_{in} = 0$  (input shorted) and  $e_1 = e_2 = e$ . If we assume  $C_{D1}$  and  $C_{D2}$  have been removed from one of the circuits, then the open circuit voltage across its terminals is:

$$e_{D1} = e_1 - \frac{C_5}{C_1 + C_5} e_2 \text{ for } C_{D1} \text{ and}$$

$$e_{D2} = e_1 - \frac{C_6}{C_2 + C_6} e_2 \text{ for } C_{D2}.$$

The source impedances are  $C_1$  and  $C_2$ , respectively. Using values of  $C_5 = C_6 = 0.5$  pf and  $C_1 = C_2 = 500$  pf and with the input shorted ( $e_i = 0$ ), the value of the output voltage is then

$$e_{oc} = \frac{C_5}{C_1 + C_5} e_2 + \frac{C_6}{C_2 + C_6} e_2 = \frac{e_2}{500} .$$

Then, using  $e_i = \frac{e_2}{500}$  for the common mode input voltage, the value for the output voltage becomes

$$e_{oc} = 2K \left( \frac{e_2}{500} \right)^2 = 8 \times 10^{-6} K(e_2)^2 .$$

The common mode ratio computed was about 54 db. Since this circuit has good sensitivity, good common mode rejection, and consists of a circuit balanced with respect to RF, it was used as the design for the detector circuit.

The selection of the video detector diode was based on the parameters of high frequency characteristics and burn-out level. The Sandia detector circuit used the 1N830A crystal video diode which is highly susceptible to burn-out (typically 2 ergs). Recently a new diode with good high-frequency characteristics and much better burn-out characteristics (as high as 10 ergs) has been developed (8). The fundamental mechanism involved in the device is the non-uniform heating of majority carriers by a spatially-applied non-uniform RF electric field. This gives rise to an electromotive force whose average component is proportional to the applied RF power. The heated carriers are termed "hot carriers," hence the name of Hot Carrier diode has been used to name the device. The diode is a more efficient rectifier at high frequencies than a pn junction-type because it does not store minority carriers during normal operation (9).

The performance of hot-carrier diodes conforms closely with theory. The low-level voltage-current characteristics can be accurately described by

the equation

$$i = I_s \left[ \exp \left( \frac{qv}{nKT} \right) - 1 \right]$$

Where  $n$  is the diode ideality factor (nominally about 1.05 at room temperature);

the other parameters are those used in the normal diode equation. Junction resistance is a function of the diode current and at 25 degrees C is described

by the equation

$$R_j = \frac{dv}{di} = \left( \frac{26}{I_s} \right) \exp \left( \frac{-v}{26} \right),$$

where  $v$  is in millivolts. The junction capacitance is given by

$$C_j = C_j(0) / \left( 1 - \frac{v}{V_b} \right)^{\frac{1}{2}},$$

where  $C_j(0)$  is the zero bias junction capacitance and  $V_b$  is the built-in potential (about 0.45 eV). Typically, the series resistance  $R_s$  is about 11 ohms, the package capacitance  $C_p$  is 0.15 pF and the package inductance  $L_p$  is 3 nH.

The tangential sensitivity in dB below one milliwatt of electrical power may be expressed as follows:

$$TS_{(dbm)} = 10 \text{ Log} \left[ \frac{5\sqrt{4kT}}{u} \frac{\sqrt{R_s + R_j}}{R_j} \sqrt{\frac{R_j + R_a}{R_j}} \right] + 10 \text{ Log} \left[ 1 + \left( \frac{f}{f_c} \right)^2 \right] + 5 \text{ Log } b \quad \text{where } f_c = \frac{\sqrt{1 + R_s/R_j}}{2\pi C_j \sqrt{R_s R_j}}.$$

Typical values of TS range from -50 dbm at frequencies of 10 GHz to -65 dbm at 0.1 GHz. This is with bias current applied and at a bandwidth of 100 KHz. As used in the voltage doubler circuit, the sensitivity was less since no bias is applied. Relating these values to the values obtained experimentally

by Sandia, the actual detector sensitivity for the breadboard circuit design should be about -30 dbm. (10). This value was attained by the breadboard model. Ferrite beads were added to the design to further isolate the RF portion of the detector from the video portion.

Signal Conditioner - The output of the detector was balanced to ground therefore requiring a differential input amplifier with a single-ended output.

Several such amplifiers are available in integrated circuit form. The one selected was an operational amplifier with an open loop gain of 60,000 available, large common-mode input-signal capability, and low DC drift (11). The closed loop gain of the amplifier is given by  $G_A = \frac{R_f}{R_s}$  and  $G_B = 1 + \frac{R_f}{R_s}$ ; where  $G_A$  and  $G_B$  are the gains referred to the two inputs A and B respectively,  $R_f$  is the normal operational amplifier feedback resistance and  $R_s$  is the input resistor used ahead of inputs A and B (see Figure 4A). Since both gains must be equal, a resistance ( $R_G$ ) was added from pin B to ground which was equal in value to  $R_s$  to obtain an overall voltage gain of one. The resulting output voltage  $V_o$  is given by the following equation:

$$V_o = V_{iB} \frac{R_f}{R_s} - \frac{R_G}{R_G + R_s} V_{iA} \left(1 + \frac{R_f}{R_s}\right).$$

Since  $R_f = R_s = R_G$  the output is then

$$V_o = V_{iB}(1) - 1/2 V_{iA}(1 + 1) = V_{iB} - V_{iA}$$

which is the desired result.

The output of the amplifier was then "peak detected" and that value held until the data processing was completed for that particular input of

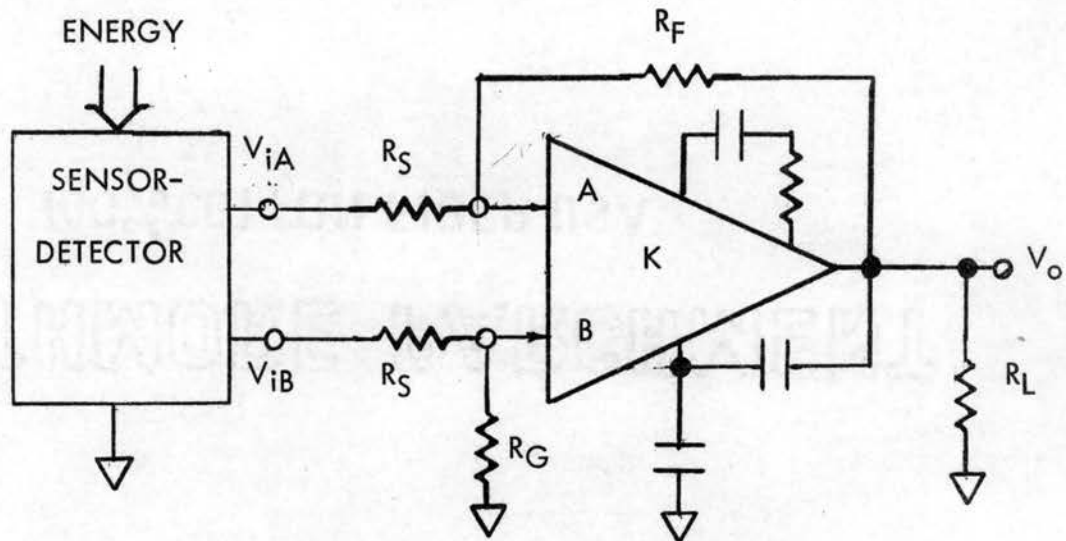


Figure 4A. Differential Input Integrated Circuit Amplifier

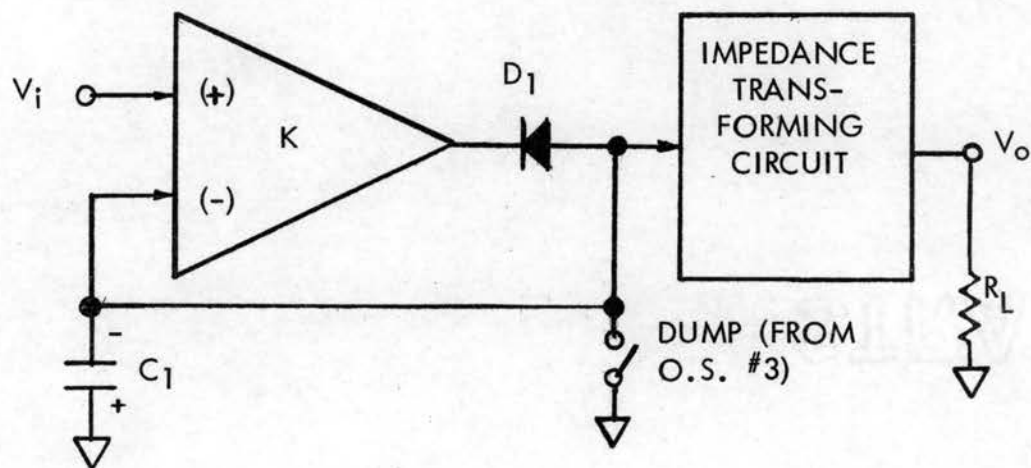


Figure 4B. Peak Detector and Impedance Transforming Circuit

energy. A peak detector using an integrated circuit amplifier was used for this function (12). The input signal was applied to the non-inverting input and the output was taken from a large capacitor connected to the inverting input (see Figure 4B). As the voltage  $V_i$  is applied, the output of the amplifier charges the capacitor rapidly through diode  $D_1$  to the peak value of  $V_i$ . When the input voltage drops below the voltage on the capacitor, the output of the amplifier swings positive leaving the capacitor charged to the peak value of the input signal. A dump circuit is used to discharge the capacitor after the data have been processed. This circuit measures the amplitude of pulses less than 100 nS wide with an accuracy of  $\pm 5$  mV. The decay time of the voltage developed across the capacitor is determined by the input bias current of the amplifier. A typical value is 20 mS/v. The maximum current drawn from the source is approximately 25  $\mu$ A. Due to the unavailability of another differential input amplifier, the breadboard model circuit consisted only of the diode and the capacitor. The input was taken directly from the sensor-detector amplifier and applied through the diode to the capacitor. The operation was the same with the exception of the difference in voltage due to the voltage drop across the diode.

The peak detector was followed by a high input impedance driver. This prevents loading of the peak detector which would otherwise decrease the voltage level before the signal could be processed by the data processor. A Darlington-type emitter follower or a high gain dc amplifier with closed loop gain of one could be used for this purpose. The effect is simply that of impedance transformation while maintaining a voltage gain of one, or nearly one in

the case of the emitter follower circuitry. The required input impedance is a function of the time required for processing the data. The RC time of the peak detector circuit must be at least 10 times the data processing time.

Since the delays of the two one-shot multivibrators used in the signal conditioner were 4 micro seconds and 136 milliseconds, this RC time was 140 milliseconds. The capacitor used in the peak detector has a value of  $1 \mu\text{f}$ ; therefore the input impedance of the transforming circuit should have been at least 1.4 megohms; however a high impedance driver was not available for the breadboard. The output impedance of the circuit should have been very low to prevent loading by the Schmitt triggers in the data processor when their input threshold voltage is exceeded. The absence of this impedance transforming circuit did not prevent the circuit from operating.

The output signal from the peak detector circuit is also applied to the input of a Schmitt trigger in the signal conditioner. The input threshold of this circuit was set to the lowest desired threshold level of the entire monitor. In effect, this performs the function of a squelch circuit in that it prevents the processing of weak noise signals which would otherwise cause the data processor to operate continuously, thus giving enormous counts of very small energy levels. Although this may be truly representative of the actual electromagnetic environment, such operation would rapidly "fill up" the data processor registers. This would seriously limit the period of time the monitor could function before saturation. Since the higher levels of energy are the most significant, the threshold of this Schmitt trigger was set at a level corresponding to a certain energy level at the input to the detector. This level

would be determined separately for each EED circuit that is to be monitored. For the purposes of the experiment, this level was set at one milliwatt of power. For the general case of monitoring EED's this level will be 40 db below the no-fire energy level of the monitored EED.

The output of Schmitt trigger in the signal conditioner provides the turn-on signal for the power switching circuit. Actually, two such circuits might be required if a plus and minus power supply is used as the final design in a production model. This circuit was not breadboarded for the experiment since it does not apply to the statistical data processor. The output of the Schmitt trigger is also applied to a one-shot multivibrator (O.S. #1). This delay would allow time for the power to be switched to the data processor circuits. The output of this delay circuit is then used to trigger another one-shot delay. The use of two delay circuits provides additional buffering and allows the data processor circuits to stabilize before the data are stored. The output of the second delay (O.S. #2) then provides the "store" pulse to the data processor and also triggers another delay (O.S. #3) whose function is to dump the voltage level held in the peak detector circuit. The delay time of the one-shot multivibrators was set to provide sufficient time for the operation of the data processor circuits. Large values of delay are not desirable in conjunction with integrated circuits because of the large values of capacitance required. Integrated circuit resistance values are normally much lower than corresponding discrete element circuits due to the properties of the substrate. An increased amount of delay could have been added to the design by the use of additional delay circuits rather than using large values of capacitance. The



signal conditioner provides both the signal level output and the store pulse to the data processor and also the signal level to the analog-to-digital converter. All of the circuits used in the signal conditioner are presently available in integrated circuit form. The combination of these circuits into a composite system would entail a custom engineering job which must be accomplished by an integrated circuit manufacturer.

Data Processor - The input signal was applied in parallel to four threshold detectors. The number four was chosen to keep the physical size of the package small while yet providing a division of data levels that will produce a rough approximation to the actual distribution. Although the number of divisions of signal level could be quite large, the number chosen demonstrated the feasibility of the design concept. If a system were designed to be laboratory or ground-based monitor rather than airborne, the tradeoffs of weight, size, cost, and complexity versus accuracy would result in a larger number of threshold detectors. Under that design criteria the number would be limited by the accuracy to which the input voltage thresholds could be set without the occurrence of overlapping levels.

The threshold detectors were designed using Schmitt trigger circuits whose switching thresholds are variable over the range of -0.5 to -2.5 volts. These voltage levels conform to standard designs that were available for use. Although the range of voltage could have been reduced, this would make the setting of the threshold level more critical than was deemed necessary.

The logic output of each detector is 1 if its threshold has been exceeded, or 0 if its threshold level has not been exceeded. The 1 output is applied to a 2-input AND gate associated with that detector. The output of the gate is applied to its associated counter. The 1 output of each detector was also applied through an inverter to become one of the 2 inputs of the preceding gate. The output of the gate is applied to the associated counter. Another input to the gated counter is the store pulse which is connected in parallel to all the gates on each counter. The logic of the design is to count only that detector which has operated on the highest level signal (13). The logic equation for this operation is

Count #1 if  $1\bar{2}S$

Count #2 if  $2\bar{3}S$

.

.

Count #7 if  $7\bar{8}S$

Count #8 if  $8S$

Where 1, 2, ..., 8 represent a 1 output of each respective detector,  $\bar{1}$ ,  $\bar{2}$ , ...,  $\bar{8}$  represent a 0 output of each respective detector, and S represents the presence of the store pulse.

The threshold counters 1 through 4 are four-stage binary counters which represent a capacity of 9 counts each. The decision to limit the number of counts to 9 was based on the availability of modules for the experiment. The criteria of low weight and volume versus the desired data capacity of the monitor would set the number of counters in a production model.

The counters were designed to be read out by interrogating each flip-flop to determine the state of 0 or 1. This was accomplished by the measurement of voltages which is the most straightforward of several available methods. This represents a serial-type read out. By application of additional AND gates and associated equipment the outputs of the counters could be dumped in parallel and then processed by automatic means using complex equipment. The nature of the read out is purely dependent on the users requirements and was not considered a part of the design problem.

All circuits used in the data processor are available in integrated circuit form and could be combined in one complex subsystem or integrated into the whole of the monitor system. The only design constraint would be that provisions must be made to bring out the outputs of all of the counters. This might represent a considerable number of leads and could require the use of an ultra-miniature connector. For the breadboard model the outputs were brought to two plug-in connectors and the outputs labeled. This facilitated the read out during the performing of the experiment.

Peak Reading Analog-to-Digital Converter (ADC) - Conversion of a signal from analog to digital form can be accomplished by several techniques.

However, the design requirement that the monitor provide an output that is the highest value of stray energy observed during the monitoring period, leads quickly to the selection of a peak reading ADC employing the counter method (14). This design is also the most straightforward and is low in cost. Several other methods that were evaluated were the simultaneous method, the

continuous method and the successive approximation method. These methods were either not compatible with the requirements to store the highest reading continuously or were more elaborate than necessary. The design selected is available commercially using hybrid thin-film microcircuits and monolithic integrated circuits for the control logic, output register, and comparator; this design requires a reference voltage supply using discrete components (15). This reference voltage supply could be a nickel-cadmium battery or mercury cells.

The ADC consists of a voltage comparator, clock, gate, counter, reference supply and a digital-to-analog converter. The heart of analog-to-digital conversion is the comparator circuit. The stray energy signal, after passing through the signal conditioner, is applied to the comparator. This circuit compares the signal with the voltage from the digital-to-analog converter (which has stored the highest voltage level processed up to that time). If the signal voltage level is higher than the stored voltage, the comparator produces an output to the gate. The clock (free-running multivibrator) output is then gated to the counter and counts as long as the gate is open. The output of the counter is applied to the digital-to-analog converter and also stored as the digital equivalent of the highest signal counted. The digital-to-analog converter applies the increasing analog voltage to the comparator and when the two voltages are equal the comparator output returns to zero, thereby inhibiting the gate and stopping the count. If the next stray energy signal is lower than the stored signal, no output is obtained from the comparator and the voltage level remains at the previous higher level. Thus the operation is

one of a peak-reading voltmeter. The counter is continuously supplied with power so that the count is never dumped out of the register during the monitoring period.

The aspects of accuracy is important when representing a given value in different terms. Several sources of error are present in any ADC. When an analog signal is quantized, there exists an error equal to the smallest quantum. In this converter the error is equal to  $\pm \frac{1}{2}$  the least significant bit. Since the thresholds are separated by the value of 0.5 volts, an accuracy of one-tenth the range should be sufficient. This amounts to 0.05 volts and represents a percentage of 2%. A 7-bit system would have a built-in error of  $\pm 0.75\%$  which represents about 1/3 or 1/2 of the total system error. Other major sources of error are the offset, calibration, and linearity of the analog comparator. Reference supply ripple is another contributing error; however, the use of a battery should remove the ripple error.

Power Switching Circuit - The decision to incorporate a second mode of operation for the power supply was based on the larger power requirements of integrated circuits compared to discrete solid-state circuit design. While the power consumption of either design is low, the long time period required and the minimum size criteria justified the additional circuit complexity in order to achieve a lower power drain. This is important for airborne applications where the power supply would be some type of battery.

The circuit is a simple series switch that is turned on by another series switch. The power switch applies power to those circuits not needed for

sensing and storing data. Continuous power is applied to the electronics that sense the incoming stray energy and that store the resultant data in the digital registers. The transistors used as switches are either on or off and do not dissipate very much power; therefore, a low power transistor would be used for this application. The power switch is operated by the output of the Schmitt trigger in the signal conditioner. Since the data are not stored until after the one-shot delays have operated, the electronics have sufficient time to stabilize after the initial surge due to the step application of power.

### System Operation

Signal Conditioner - The signal conditioner is used for data sampling of voltage obtained directly from the crystal diode detector (see Figure 5). The signal input is amplified and the peak amplitude held temporarily in the peak holding circuit. This is required to allow time for data processing and digitizing by the ADC (see Figure 6). The Schmitt trigger is used to sense the minimum threshold required of a data sample to be counted.

When a data sample of sufficient amplitude is received at the Schmitt trigger, the power supply is signalled to switch power to the data processing circuits. Also, the output of the trigger operates the first one shot multi-vibrator (O.S. #1). The delay times of O.S. #1 and O.S. #2 allow all of the threshold detectors of the data processor (Figure 7) to stabilize before the "store" pulse from O.S. #2 is applied to the counter gates. The output pulse of O.S. #3 "dumps" the voltage stored in the peak detector circuit, preparing it for the arrival of new data. The timing of the data processor is shown in Figure 8.

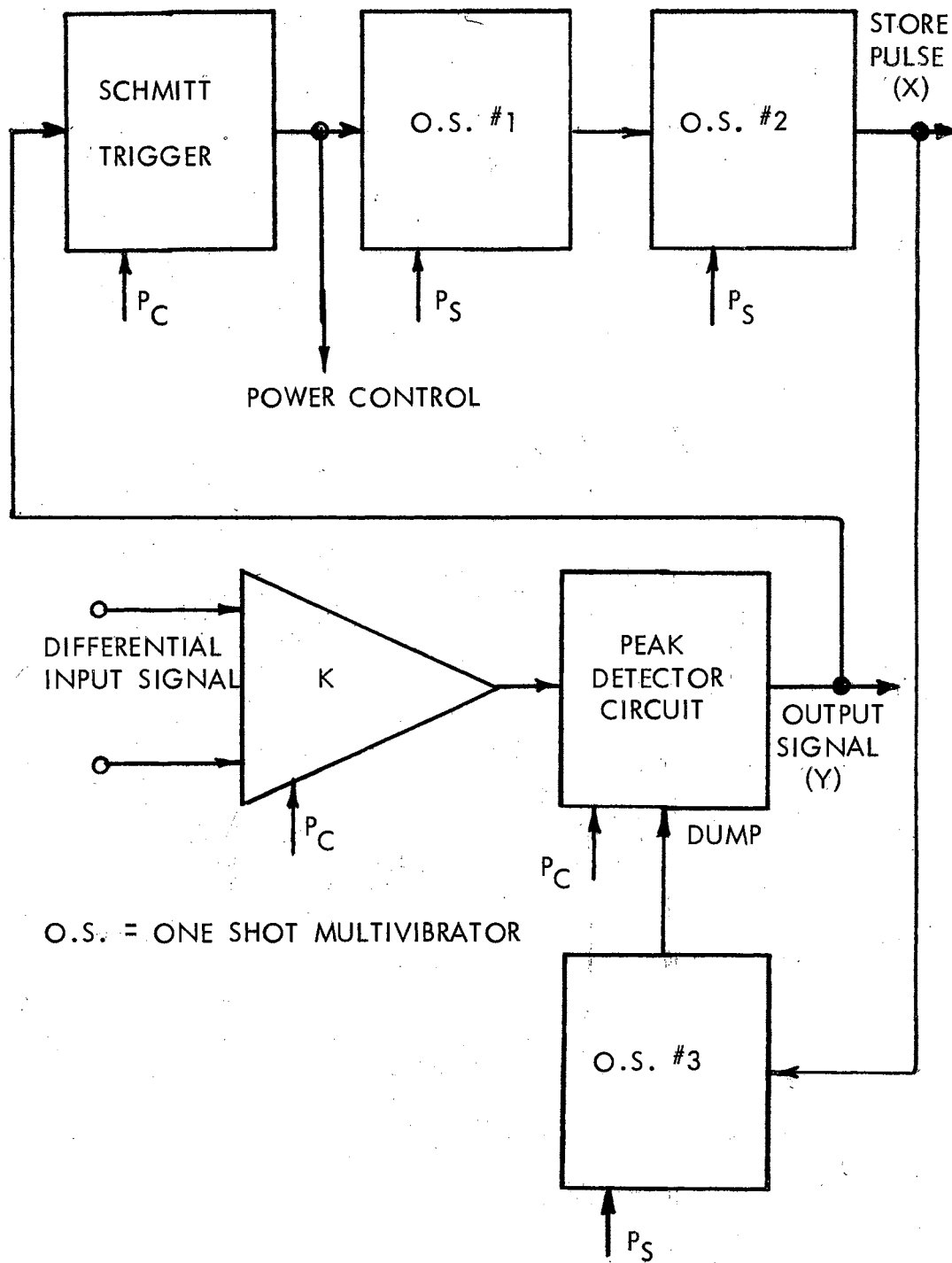


Figure 5. Signal Conditioner Block Diagram

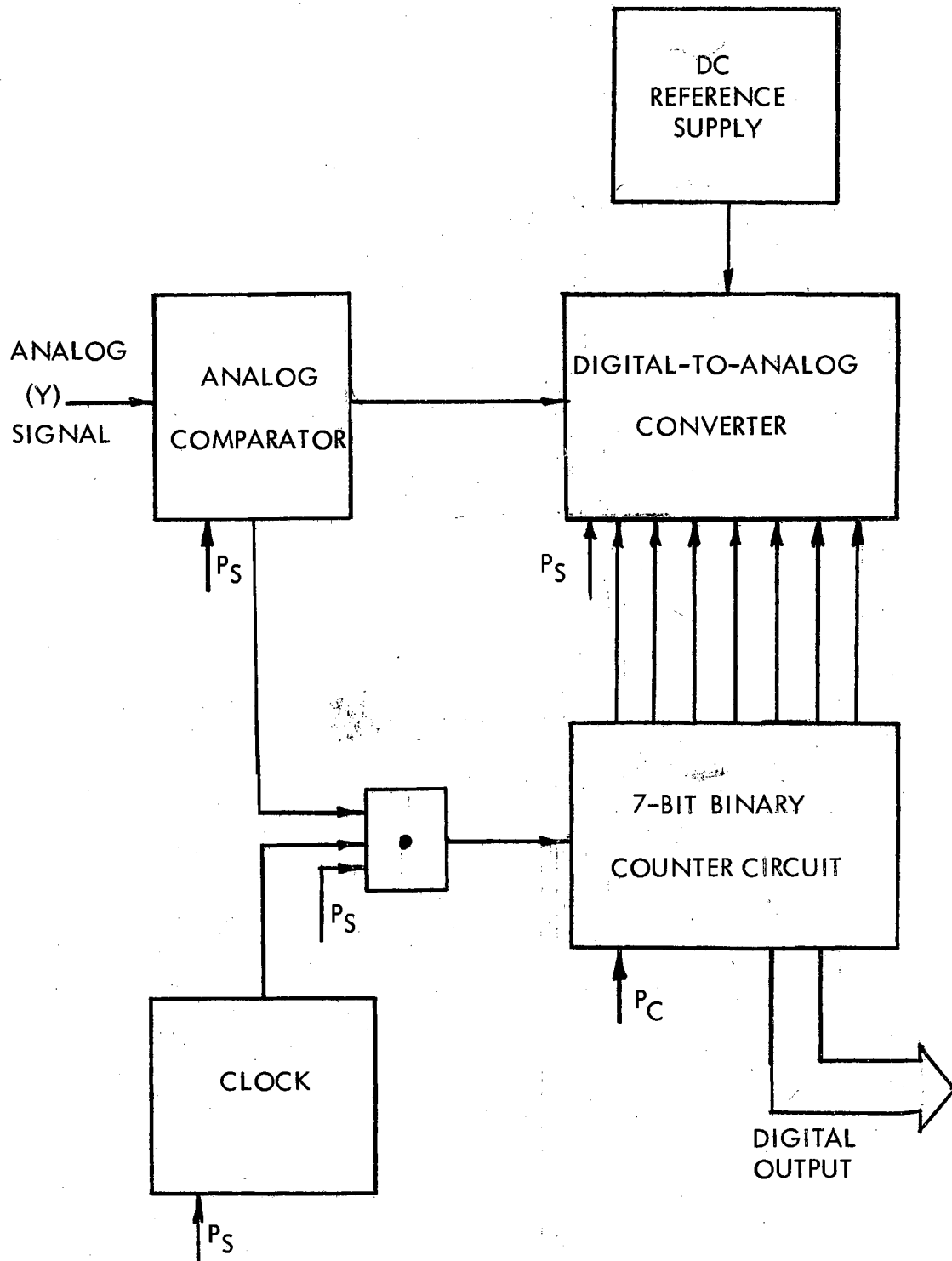


Figure 6. Analog-to-Digital Converter (ADC) Block Diagram



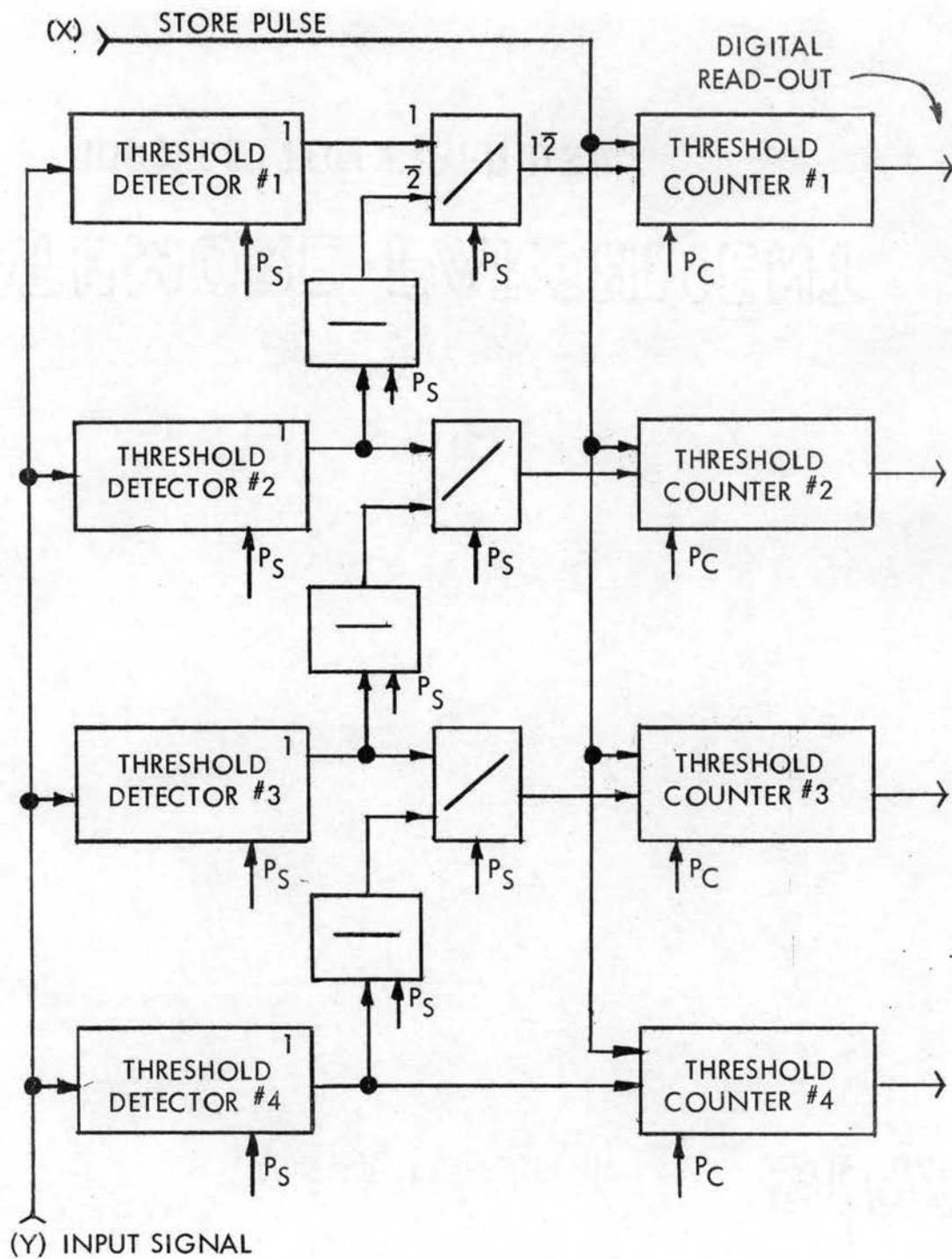


Figure 7. Data Processor Block Diagram

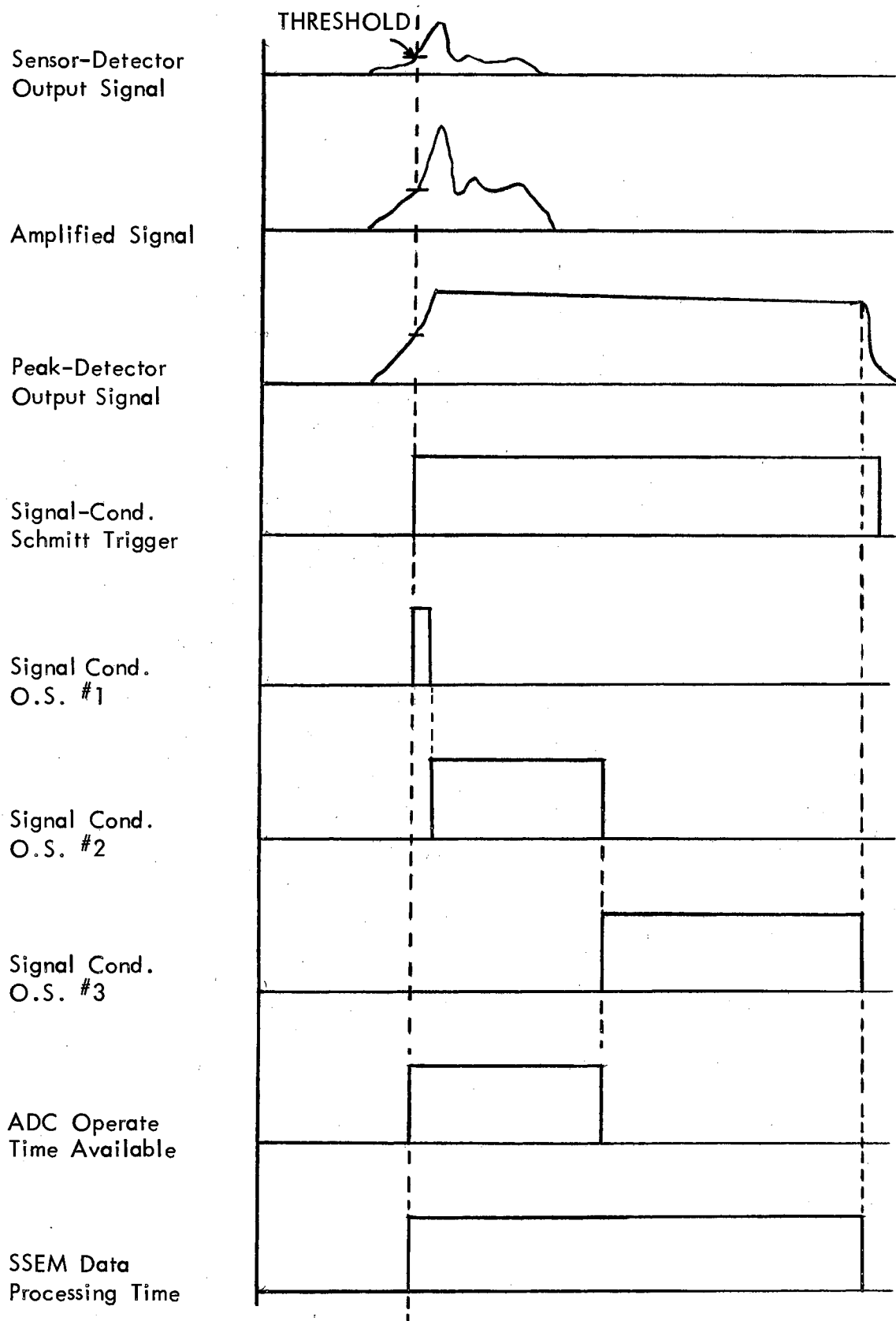


Figure 8. Timing Diagram (SSEM)

Data Processor— The input signal to the data processor is monitored by the threshold detectors (Schmitt triggers). All of the detectors with a threshold sensitivity equal to or less than the input signal will operate. Of those threshold detectors that operate (trigger), only the detector that had the highest voltage level applied will be counted. The logic gates determine which detector is the "highest." Lower valued threshold counters would "race" with each other if the processor were not timed properly. This would cause erroneous counts in the lower threshold counters. Because of this, a store pulse is applied only after the detectors stabilize, thereby precluding ambiguous data counts.

The threshold detectors are set to trigger at equally spaced intervals of increasingly higher voltage. The logic gates permit only the highest valued threshold detector to load its respective threshold counter. The counts stored in the threshold counters are an approximation of the distribution of the data. The stored data were read out by use of a voltmeter rather than automatic serial or parallel dumping of the data into a recorder or other storage device. These data were then used in later analysis.

Analog-to-Digital Converter (ADC) — The ADC is a "level at a time" converter which consists of a clock, a comparator, a summing network, and a binary counter. It operates as a peak-reading voltmeter which stores the signal of greatest amplitude that was encountered during the test period. The clock is a free-running multivibrator which drives the ADC. The comparator is in the feedback loop of the ADC and determines whether the digital value

in the binary counter is equivalent to the input signal. When this occurs, the digitizer stops due to the inhibiting of the "AND" gate, thereby stopping the clock pulses from driving the binary counter. The summing network converts the digital value of the binary counter to an analog voltage (D to A converter). The binary counter determines the digital equivalent of the input signal and stores this value for later readout. When new data samples occur later, that have a value greater than the stored level, the binary counter begins counting because the comparator signals the AND gate to start the clock. The ADC was not breadboarded since a commercial version was available for the operation of the experiment.

Power Supply - The power supply has two types of output; switched power ( $P_s$ ) and continuous power ( $P_c$ ). The electronics necessary to determine when a signal is present and to store data have power applied continuously. The other circuits have power applied only during data processing periods. Power switching is necessary in order to conserve battery power during the long data sampling period. Power switching also eliminates some of the gating hardware necessary to isolate various circuits from one another. A simple series power switch is used to control the power (see Figure 9A). This switch is controlled by the threshold detecting Schmitt trigger located in the signal conditioner.

Sensor-Detector - The detector converts the RF voltage into video voltage. A crystal diode detector using the voltage doubler principle is shown in Figure 9B. The use of hot carrier diodes provides the detector with good

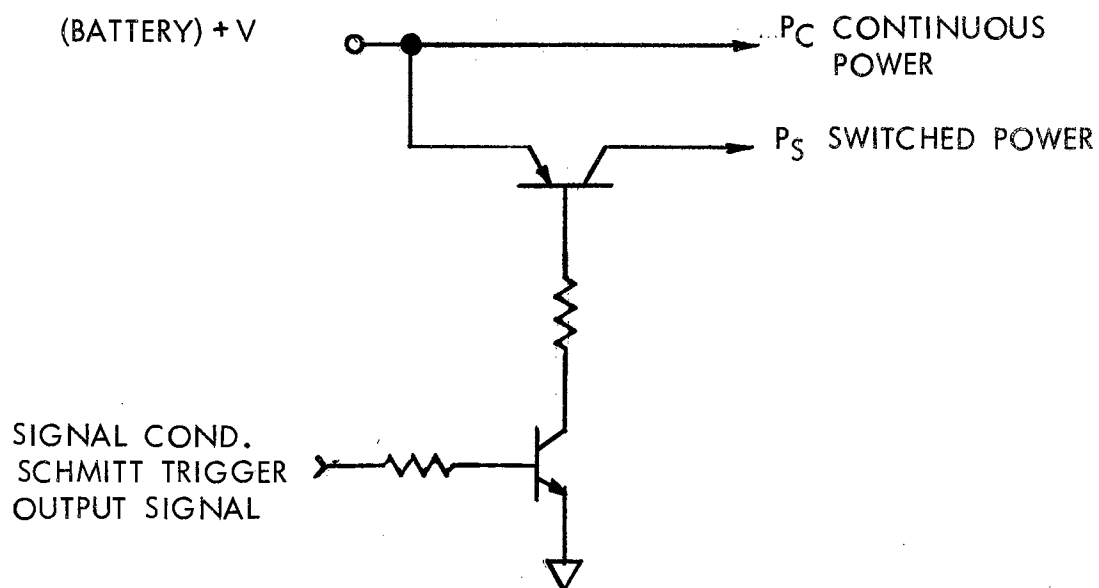


Figure 9A. Power Switching Circuit

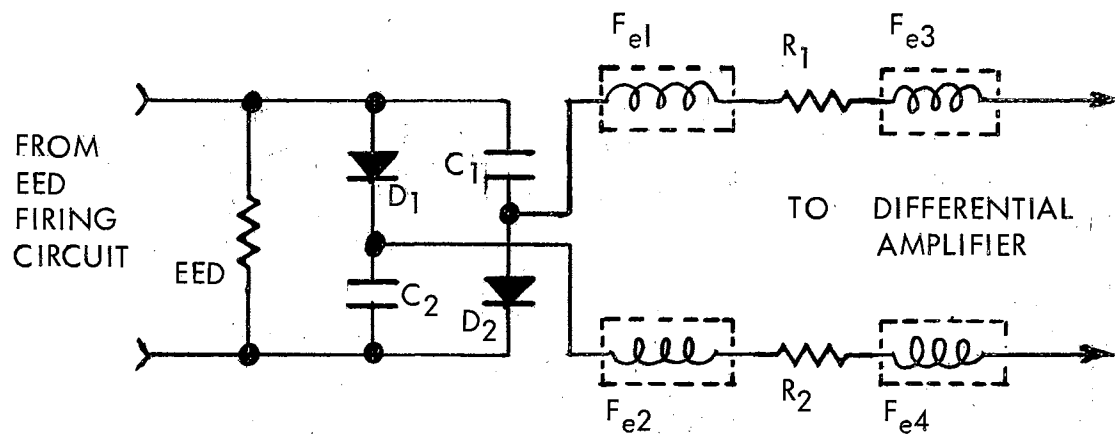


Figure 9B. Sensor-Detector Schematic Diagram

frequency sensitivity and a high burnout rating. The following design objectives were established for the detector:

1. Tangential sensitivity (CW) 35 db below one milliwatt of electrical power
2. Frequency range (3 db points) 14 KHz to 10 GHz
3. Dynamic range  $>$  80 db
4. Video bandwidth 1.0 MHz
5. Self-powered with  $>$  60 db common mode rejection.

The best sensitivity obtained was 30 db below one milliwatt rather than 35 db. The frequency range objective was met with only 6 db variations across the band. The dynamic range could only be measured up to 56 db since higher powered signal generators were not available. The video bandwidth was easily met since the differential amplifier following the detector was not bandwidth-limited. The common mode rejection was only 54 db.

#### Fabrication of Breadboard

In order to demonstrate the feasibility of the design concept the system was breadboarded to check functional operation. Those circuits already available in microcircuitry were modeled using commercial modules of the discrete form. The major task was the breadboard design of the sensor-detector and portions of the signal conditioner since these circuits have not been developed using microcircuits.

Digital Equipment Corporation has available a 10-bit analog-to-digital converter (Type A-801) using monolithic integrated circuits. This converter

has a built-in reference supply and is contained on one double logic module. By the use of a battery the package size could be reduced to a much smaller size. Since this subsystem is already in production, no demonstration of functional feasibility was considered necessary; therefore, an available ADC was used during the experiment.

The data processor is a new design, actually a different arrangement of standard logic modules; therefore, it was breadboarded to demonstrate the design feasibility. The logic modules, (gates, flip-flops, Schmitt triggers) were commercially available in integrated circuit form. By choosing a compatible design, there would be no interface problems. Since the electrical performance of each integrated circuit logic module was the same as those developed using discrete components, the data processor was breadboarded using Digital Equipment Corporation (DEC) hardware available at Oklahoma State University. The number of threshold levels was limited to four since this was considered sufficient to demonstrate feasibility. Since each gate requires an input from only two Schmitt triggers, a greater number of threshold detectors would simply be redundant as far as the logic operation is concerned.

The type of flip-flop used for the counters was a DEC type R202 dual flip-flop and did not require additional gates to perform the up-counter operation. The binary decimal code chosen was the 8421 code because it allowed the use of the input gates on the flip-flops (see Figure 10). The store pulse was then applied to the input of the counter gates thereby deleting the need for a 3-input gate.

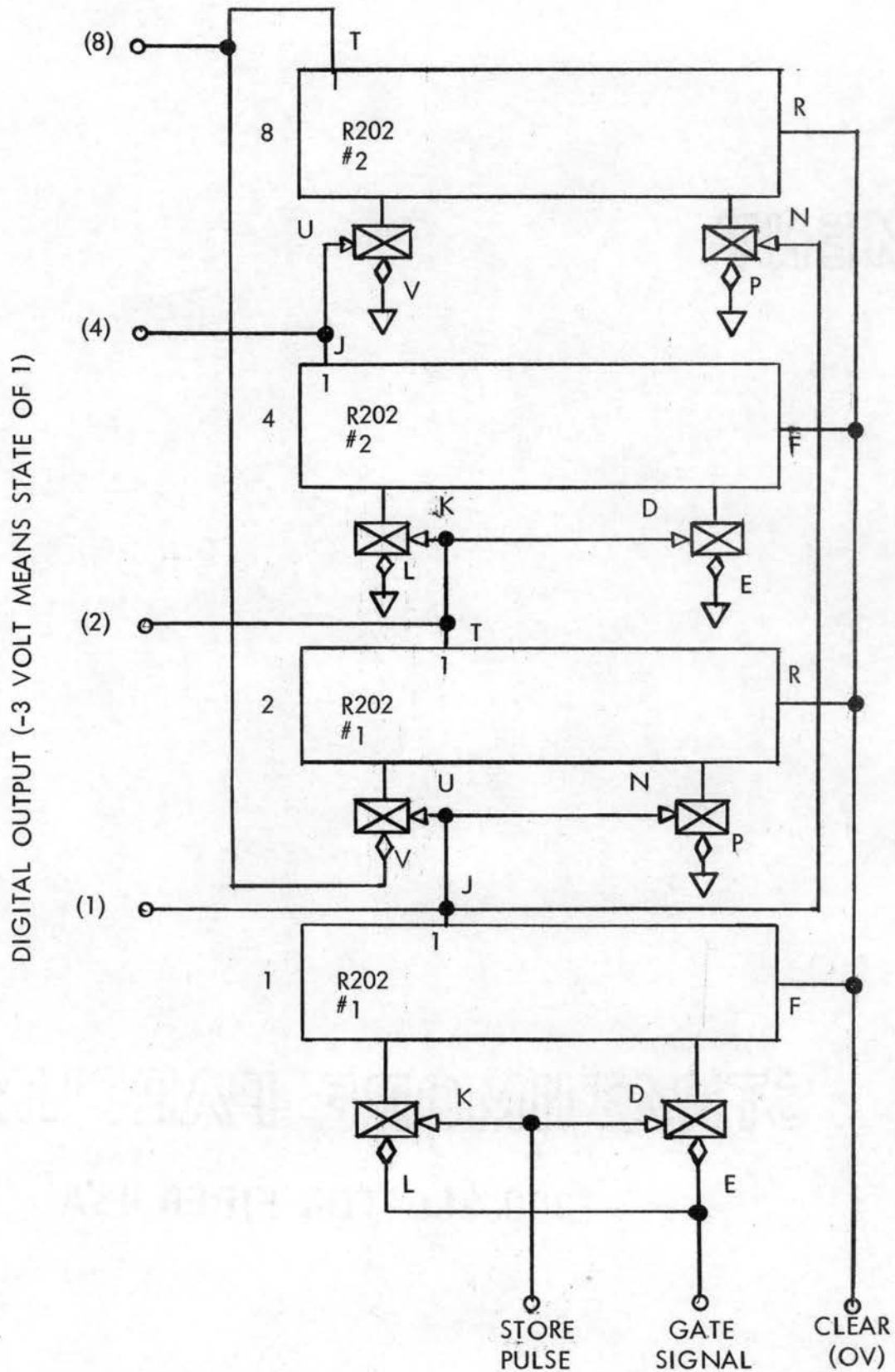


Figure 10. 8421 Up Counter Connection Diagram



The logic gates were composed of NAND gates and inverters. The NAND gate is a DEC type R111 which has 3 gating circuits on the module card. The required input logic to give the AND operation for the circuit is to have one input and not the other input.

The threshold detectors are Schmitt triggers using the DEC type W501 logic module, one circuit per module. The threshold level voltages were generated by the use of reference diodes for each of the desired threshold levels. All of the modules for the data processor were connected together in a DEC type H900 mounting panel which has a built-in +10 volt and -15 volt power supply. This provided a convenient package for the breadboard model (see Figure 11).

Portions of the signal conditioner were breadboarded using discrete logic modules. The threshold detector and the incremental delays were designed using a DEC type W501 Schmitt trigger and DEC type R302 one-shot multi-vibrators. The Schmitt trigger was set at the lowest threshold level which was -0.55 volts. The one-shot delays were set at 4 microseconds, 136 milliseconds, and 200 milliseconds delay to ensure sufficient time for Schmitt trigger operation and the discharging of the peak detector circuit. A Tektronics oscilloscope was used to observe operation of the switching times. The threshold detector and the delay modules were assembled onto the mounting panel with the data processor (see Figure 12). The amplifier and peak detector were breadboarded on a low-loss dielectric perforated board using integrated circuits and discrete components. A one microfarad capacitor was used in the peak detector circuit to ensure little droop of the signal level

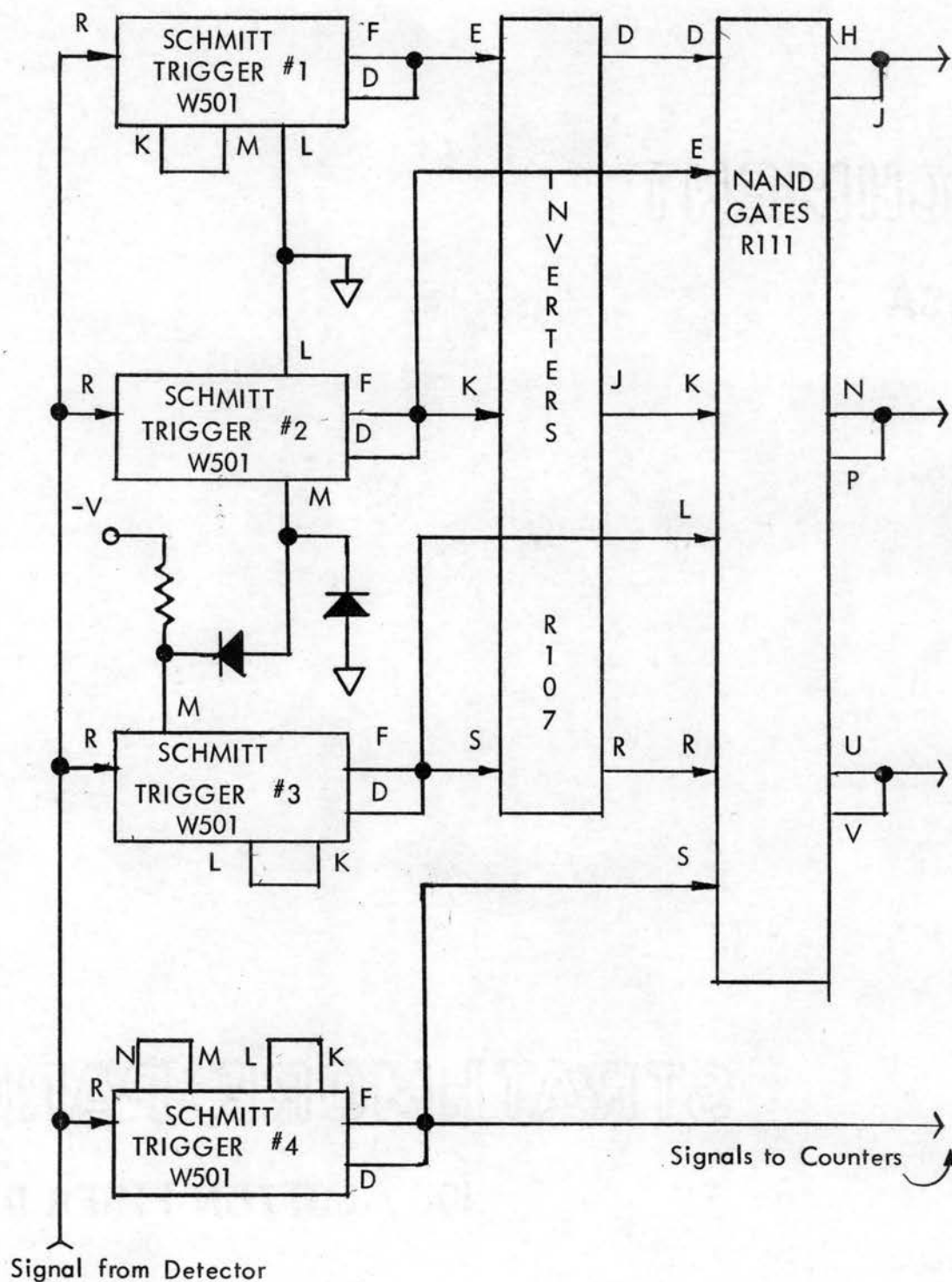


Figure 11. Threshold-Count Logic Connections

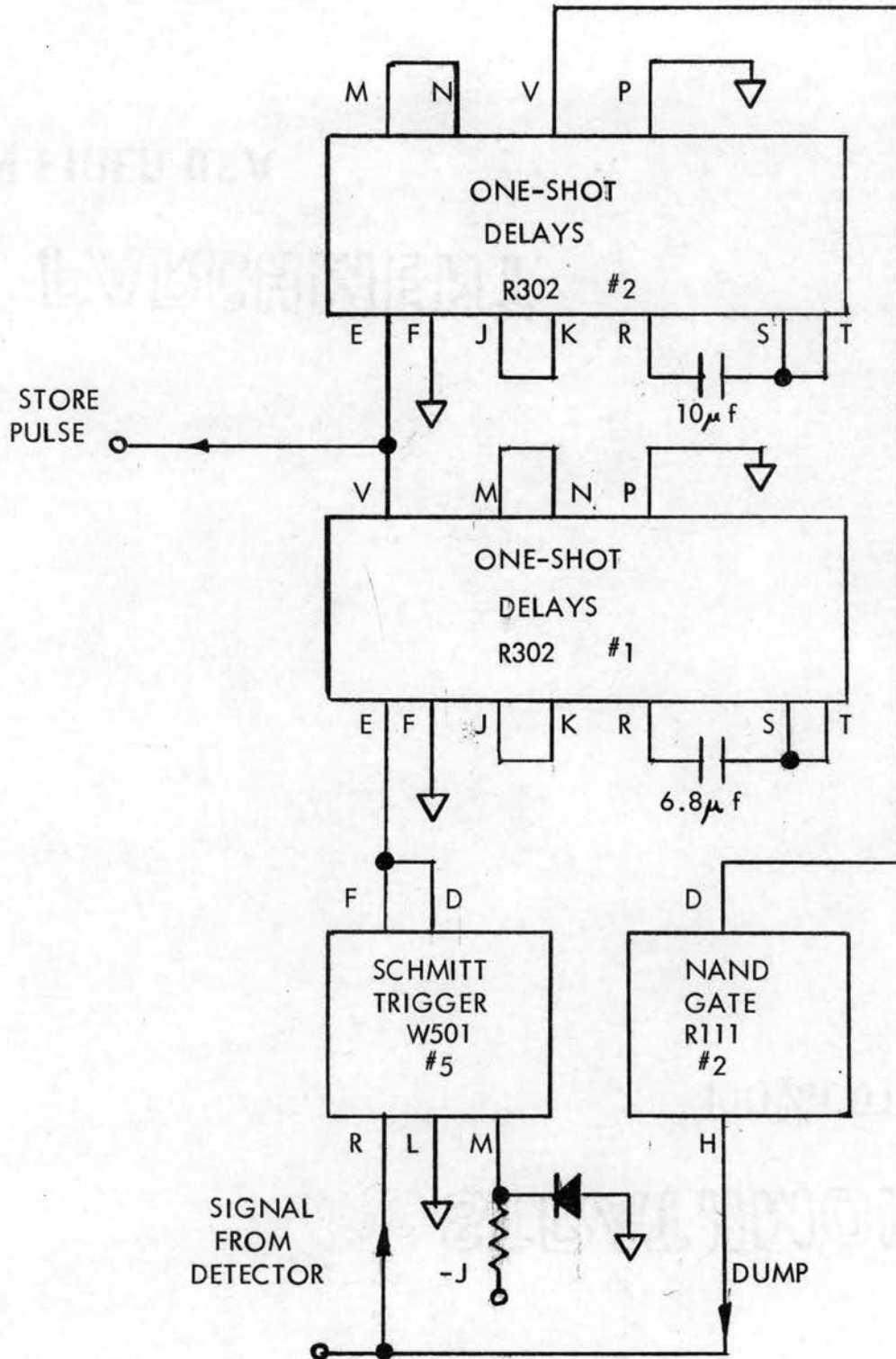


Figure 12. Timing Circuit Connections

during data processing. The amplifier was built using a Motorola MC1433 operational amplifier. The gain was set at 20 to enable the output to be visible using the low-gain head on the oscilloscope. The input to the amplifier was differential and the output single-ended. Since the load on the amplifier was capacitive, frequency compensation was necessary to prevent oscillation at the higher frequencies. A 10 picofarad capacitor from the output back to the phase lag network was necessary. Also, a 47 picofarad capacitor was connected between the lag network and ground. This eliminated the troublesome high frequency oscillation.

The sensor-detector was breadboarded on the board with the amplifier to maintain short lead wires. A pair of Hewlett Packard Associates type 2603 hot-carrier diodes were used as the non-linear elements. These were in the standard glass package; however, their incorporation into an integrated circuit package along with other components is feasible according to their applications department (16). This diode is a metal-silicon Schottky-barrier diode optimized for use as a detector from low frequencies through 10 GHz.

The capacitors used in the detector circuit were 470 picofarad type CK1MW471K from the Chem-electro Research Division of the Potter Company. A newer capacitor type 2000-471K was discussed with their representative that has a better frequency characteristic than the other type. These were back-ordered but not received in time for the experiment. The CK1MW type capacitor is a micro-miniature epoxy-dipped axial capacitor using gold-plated kovar ribbon leads.

A pair of 10K ohm resistors was used for isolation between the diodes and the amplifiers. These were one-tenth watt carbon resistors coated with ceramic. Two ferroxcube beads were placed on the resistor leads between each diode and the resistor body to filter any high frequency leakage around the diodes. These beads were obtained from the Ferroxcube Corporation (#56-590-65/3B) and are composed of high-permeability ferrite. The beads present a high series resistance to the higher frequencies and increased absorption loss. A 50 ohm Filmohm Corp. type FD 500-076 concentric disc resistor was used at the input to present a matched load to the signal generator used during tests. The sensor-detector was built inside a type N connector to eliminate losses due to radiation and to reduce the inductive resistance due to long lead lengths. The 50 $\Omega$  matching resistor, diodes, capacitors, ferroxcube beads and 10K ohm resistors were placed inside the connector and the output was brought out immediately to the input of the amplifier. This completely shielded the super high frequency portion of the monitor. The sensor-detector had previously been assembled on standoffs on the amplifier board and used a length of coaxial line to connect to the signal generator. This was all right for the lower frequencies but too lossy at the higher frequencies. Table I lists the parts used for the breadboard model.

TABLE I  
MATERIAL LIST FOR BREADBOARD MODEL

<u>DESCRIPTION</u>	<u>MANUFACTURER</u>	<u>PART NUMBER</u>
(2) capacitor, 470 pf	Chem-Electro Research	CK1MW470K
(1) capacitor, 1 $\mu$ f	Sprague	Type 150D
(1) capacitor, 0.1 $\mu$ f	Sprague	Type 150D
(1) capacitor, 10 $\mu$ f	Sprague	Type 150D
(1) capacitor, 6.8 $\mu$ f	Sprague	Type 150D
(1) capacitor, 10 pf	Aerovox	Ceramic
(1) capacitor, 47 pf	Aerovox	Ceramic
(2) diode, germanium	Sylvania	T12G
(1) diode, silicon	Sylvania	1N116
(1) diode, silicon	General Electric	1N295
(2) diode, Hot-Carrier	Hewlett-Packard Assoc.	hpa 2603
(2) resistor, carbon	IRC	1 Kohm, 1/10 watt
(3) resistor, carbon	IRC	10 Kohm, 1/10 watt
(4) resistor, carbon	IRC	100 Kohm, 1/8 watt
(1) resistor, carbon	IRC	10 ohm, 1/8 watt
(1) resistor, carbon	IRC	3 Kohm, 1/2 watt
(1) resistor, carbon	IRC	1 Kohm, 1/2 watt
(1) resistor, concentric	Filmohm	50 ohm, FD 500-076
(4) ferrite bead	Ferroxcube Corp.	56590-65/3B
(1) A-to-D converter	Electronic Engng. Corp.	EECO 761A
(1) amplifier, integrated circuit	Motorola	MC 1433
(1) connector	Amphenol	Type N
(1) power supply & panel	Digital Equip. Corp.	H900
(3) one-shot delay	Digital Equip. Corp.	R302
(5) Schmitt trigger	Digital Equip. Corp.	W501
(5) NAND gate	Digital Equip. Corp.	R111
(3) inverter	Digital Equip. Corp.	R107
(16) flip-flop	Digital Equip. Corp.	R202

## Checkout and Calibration

The sensor-detector was first checked out and calibrated using a General Radio signal generator over the frequency range from 14 KHz to 50 KHz. This generator had sine wave modulation available internally but not pulse modulation. A total of 100 millivolts was available at the output of an attenuator. A direct connection provided 2 volts output but could not be used for calibration since it bypassed the output attenuator. The sensitivity of the oscilloscope was too low to check the tangential sensitivity of the detector alone; therefore, the sensitivity measurements were made at the output of the signal conditioner amplifier. A General Radio oscillator was used for the range of frequencies from 50 MHz to 250 MHz. Again calibration was not possible because of the lack of a variable attenuator usable at that frequency range. The output of this generator was CW only. The frequency range of 250 MHz to 970 MHz was covered using a different model of a General Radio unit oscillator. The signal out of the detector varied as each generator was tuned across its band. This was due to signal generator variances and the long lead lengths used on the first sensor-detector breadboard. These variations were not present at the lower frequencies. This variation was reduced considerably when the sensor-detector was mounted inside the Type N connector.

No signal generator was available over the frequency range from 970 MHz to 7.0 GHz. The detector was then checked over the frequency range of 7.0 GHz to 11 GHz using a Hewlett-Packard signal generator. This generator had both square wave and pulse modulation. A calibrated attenuator was

built-in so that tangential sensitivity measurements could be made across the frequency band.

The amplifier of the signal conditioner was built with a gain of 20 instead of one as originally planned to help alleviate the low-gain problem. After much reading of the application notes and some phone calls to Motorola, the reasons for the high frequency oscillations of the amplifier were discovered and eliminated. By using the amplifier connected to the output of the detector, and a highly sensitive vacuum tube voltmeter, the circuit was calibrated.

The modules for the rest of the signal conditioner and the data processor were checked out after their connection in the mounting panel. The only adjustments necessary were the threshold level of the Schmitt triggers. These were checked using a vacuum tube voltmeter on the input and observing the output with a scope. The analog-to-digital converter used was a self-contained instrument and did not require calibration.

The most difficult part of the calibration was the calibrating of the sensor-detector. A high-gain sensitive head was needed on the oscilloscope. A variable attenuator and pulse-modulated, high-output signal generators were certainly needed. The following tangential sensitivities were measured for the sensor-detector using the amplifier to provide enough gain and a higher gain head on the oscilloscope:

- (1) 14 KHz - 75 db below one milliwatt of electrical power,
- (2) 50 MHz - 55 db below one milliwatt of electrical power,



(3) 7.0 GHz - 30 db below one milliwatt of electrical power, and

(4) 11.0 GHz - 27 db below one milliwatt of electrical power.

The test equipment used for checkout, calibration, and during performance of the experiment test is shown in Table II.

TABLE II  
LIST OF TEST EQUIPMENT

<u>DESCRIPTION</u>	<u>MANUFACTURER</u>	<u>MODEL NUMBER</u>
DC Vacuum tube voltmeter	Hewlett-Packard	HP 412A
DC Power supply	Hewlett-Packard	HP 721A
Signal Generator	Hewlett-Packard	HP 620A
Oscilloscope	Tektronic	Type 561
Signal Generator	General Radio Co.	Type 1001-A
Unit Oscillator	General Radio Co.	Type 1208-B
Unit Oscillator	General Radio Co.	Type 1209-B
Unit Power supply	General Radio Co.	Type 1203-B
Pulse Generator	Rutherford Electronics	Model B7B

## CHAPTER IV

### EXPERIMENTAL TEST DATA

#### Treatment of Test Data

The purpose of the SSEM is to monitor stray electromagnetic energy of varying frequency, amplitude and duration. This stray energy constitutes an electromagnetic environment which was simulated to check the operation of the SSEM. This environment was simulated by using the output signal from a General Radio type 1001-A signal generator.

Since the total count capacity of each counter register is nine, it was felt necessary to conduct more tests than originally planned; therefore, the simulated environment was applied a large number of times and the resulting count taken from each of the four counters was summed. This statistically achieves the same result as if there were a larger number of flip-flops which would give the SSEM a large capacity counter register.

The division of threshold levels is four; therefore, the resulting data did not give a nice, smooth distribution curve but a rather rough one. Nonetheless, it demonstrated that a distributional form was available from the SSEM.

The output of the ADC is simply the peak voltage level applied to the data processor during the test period. Although the upper limit on the threshold detectors was -2.5 volts, the ADC read the peak voltage applied. This

voltage level could have been the saturation level of the signal conditioner amplifier which was  $\pm 8$  VDC for the breadboard model.

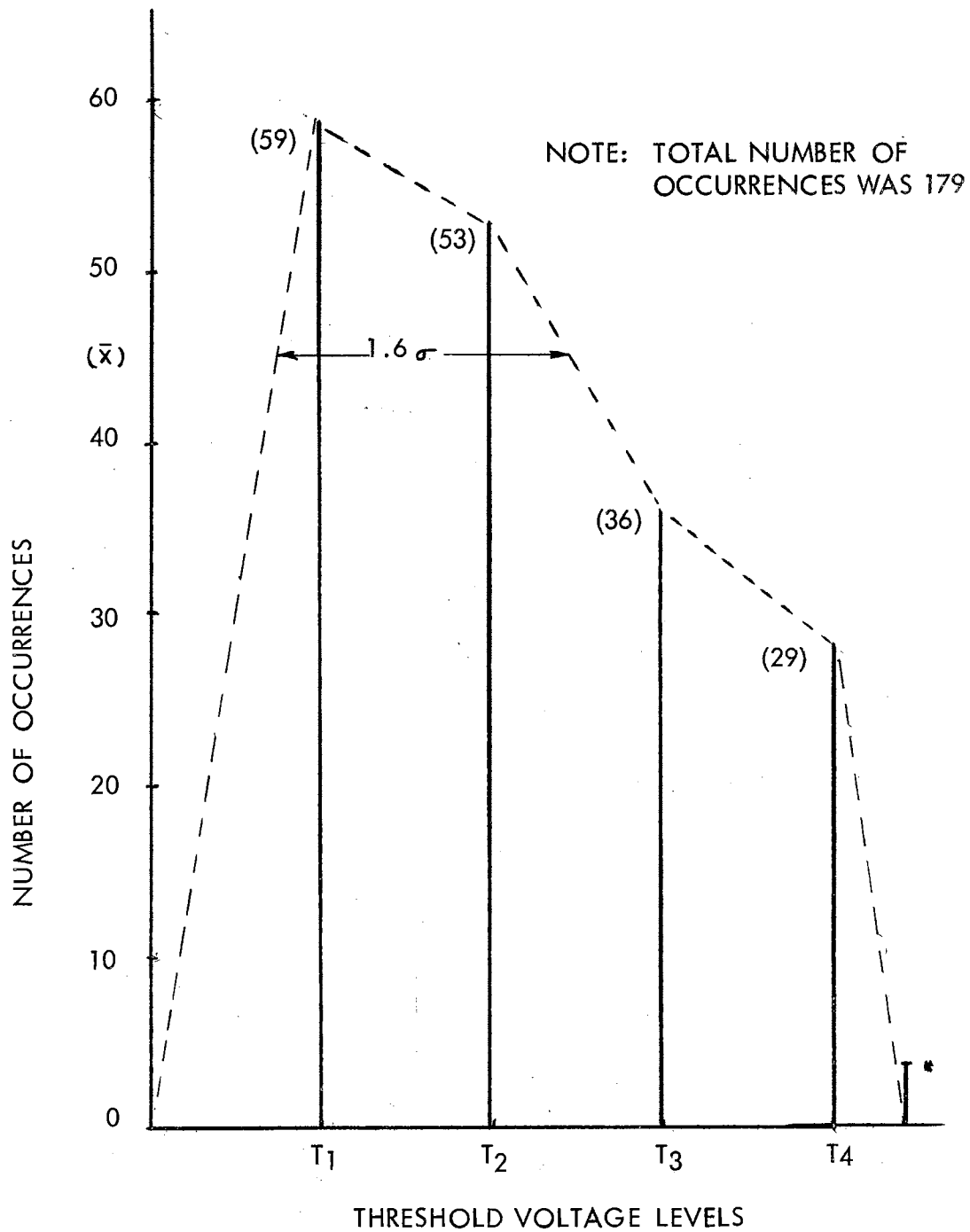
The output of the signal generator was varied randomly during each test. A different frequency was selected at random for each succeeding test. The length of each sampling period (test) was approximately 10 seconds. This was to allow sufficient time for the counters to run up a sizeable count. The count for each counter was read out by a voltmeter and recorded. (See Table III). A total of 100 tests or sampling periods were conducted during the experiment. These periods were randomly divided into groups of ten and the counts for each of the ten test groups were summed for each counter. These number of occurrences were plotted as a function of voltage level to obtain a graph of the data distribution (see Figure 13). The highest value of voltage was read from the ADC during each sampling period and these were averaged for each group of ten sampling periods. The highest level was then recorded as the highest voltage level encountered during the entire sampling period. The total number of occurrences was then calculated and entered as such on the graph.

#### Correlation With Design Analysis

The best correlation was obtained for the frequency response of the sensor-detector which performed well up to and including 11 GHz. No correlation was attempted for the power handling capability of the hot carrier diodes since it was not possible to procure additional matched pairs for the experiment in case of burn-out. The tangential sensitivity measured at

TABLE III  
TEST DATA OBTAINED DURING SAMPLING PERIOD

COUNTER #				COUNTER #				COUNTER #			
1	2	3	4	1	2	3	4	1	2	3	4
<u>GROUP #1</u>				<u>GROUP #4 (Cont'd)</u>				<u>GROUP #7 (Cont'd)</u>			
9	9	7	0	7	8	5	0	8	6	6	3
8	7	3	5	7	4	1	2	7	3	2	2
7	3	4	2	5	9	2	5	7	6	1	1
6	5	2	2	2	3	6	2	6	7	5	4
8	7	6	0	8	6	6	3				
5	8	3	6	9	1	3	1	<u>GROUP #8</u>			
8	9	4	3	9	1	5	5	4	8	0	2
8	9	5	6	<u>GROUP #5</u>				5	2	1	1
6	0	5	5	9	1	6	8	6	7	4	3
4	3	3	2	9	6	5	2	4	2	1	1
<u>GROUP #2</u>				5	9	1	6	7	0	6	4
4	4	2	8	6	7	3	2	7	8	6	2
8	1	2	0	0	2	5	1	6	8	1	5
6	7	4	5	6	5	2	1	6	2	2	6
0	0	4	4	4	2	2	1	7	8	2	5
8	6	4	2	4	4	6	1	6	0	4	4
1	5	6	1	8	2	3	1	<u>GROUP #9</u>			
3	7	1	2	5	0	3	4	3	6	8	3
0	5	6	3	<u>GROUP #6</u>				7	6	1	3
9	6	4	3	9	9	2	2	7	3	2	2
0	3	4	2	9	6	6	1	8	9	6	6
<u>GROUP #3</u>				8	8	6	5	2	4	6	2
8	8	1	5	6	4	4	3	9	6	6	1
8	0	5	5	8	1	4	6	4	3	1	1
0	6	6	4	3	9	1	1	4	9	3	3
9	7	6	0	1	6	6	4	7	7	3	2
9	9	6	4	3	9	2	5	7	9	1	3
9	0	3	4	8	2	4	1	<u>GROUP #10</u>			
5	7	2	3	6	9	2	3	4	2	8	8
6	2	4	1	<u>GROUP #7</u>				5	8	1	3
8	4	6	2	7	2	7	7	5	7	1	4
3	8	1	3	8	6	3	2	7	7	1	6
<u>GROUP #4</u>				8	8	4	3	7	8	5	0
4	7	3	1	7	8	4	3	2	8	6	5
6	7	2	4	9	8	2	2	5	9	2	1
6	8	1	3	7	9	2	0	6	7	1	4
				7	0	2	4	9	3	4	1
								0	4	4	3



\*PEAK READING VOLTMETER VALUE WAS 3.1 VOLTS

Figure 13. Plot of Actual Data Distribution  
During Test Monitoring of Stray Energy

several discrete frequencies was less than calculated during the analysis; however, this was only 5 db lower. The difficulty encountered during packaging of the detector was perhaps responsible for this. A more thorough development of the physical layout of the detector would be necessary to overcome this deficiency.

No problem was encountered with the logic portion of the monitor since it was very straightforward using well-developed logic design. The logic modules used were all from one company and no scaling or buffering was necessary which was a tremendous asset. The functions of the data processor therefore correlated well with the design analysis.

## CHAPTER V

### RESULTS AND SUMMARY

#### Discussion of Test Results

The results of the experiment tests show that the largest number of occurrences happened at the lower voltage levels for the simulated environment. The distribution of voltage levels has a  $1.6\sigma$  spread at the 50 percentile frequency-of-occurrence which was calculated to be 44.48. The arithmetic mean for the sum of all the counters was 44.7 which was very close to the 50 percentile of the number of occurrences. This nearness was probably due to the method of applying the random voltage levels. Since the voltage level was changed by physically varying the attenuator on the signal generator, the SSEM was no doubt counting as the voltage level decreased. A better test would have been the step application of discrete voltage levels rather than the slowly varying voltage obtained by manual manipulation of the attenuator. The results were sufficient to show the method of statistical determination of the electromagnetic environment.

#### Summary and Conclusions

The feasibility of the SSEM concept was demonstrated during this investigation. The system was designed using circuitry that is adaptable to integrated

circuit construction techniques. In fact, a great many of the functions are already developed in integrated circuit form. The recent development of hot-carrier diodes made it possible to use a crystal-diode-detector design (for non-interference with the system that is being monitored) that has high burn-out resistance. The likely presence of large magnitude signals made this most desirable.

At the beginning of the project it seemed that sensitivity requirements would have to be relaxed; however, the hot carrier diodes performed very well and did not require pre-biasing to achieve the desired tangential sensitivity. As the design is now, the limits on sensitivity are imposed by the available dynamic range of the amplifiers following the detector. The monitor as designed has a limited dynamic range imposed by the threshold-level range of the Schmitt triggers. By using scaling techniques and offset-voltage reference levels, this limitation could be removed. This would be a good follow-on project.

The author has found that while integrated circuits are desirable from the standpoint of size and weight, they do require a larger standby power making it necessary to incorporate a power switching circuit to conserve battery power. This was not readily apparent at first. Also, the design at present requires a large number of interconnection points for read-out of the stored data. Automatic means of reading out the data in serial rather than parallel would alleviate this problem.



Now that the concept feasibility has been proven, the next logical step would be to develop the SSEM completely in integrated circuitry. The first subsystem requiring this development is the sensor-detector. From a physical standpoint this circuit may be separated from the rest of the monitor. A small, thin wafer inserted between the EED and its mating connector is desired for the application of the monitor to a real electroexplosive system. The sensor-detector would be located on this wafer with perhaps an amplifier to act as a line driver. This task constitutes the major challenge as the rest of the circuitry is most straightforward. It is believed that this would also be the most interesting part of the design problem since it involves working with super-high frequencies and low-frequency video on the same integrated chip.

## BIBLIOGRAPHY

1. Mulkey, Owen R. "A Thin Film Micro-Thermocouple RF Energy Detector for EED Wiring." Boeing Company, Seattle, Washington. IEEE Transactions on Aerospace (Supplement) June 1965 pp 647-651.
2. Hewitt, J. G. et al. "Vacuum Deposited Thermocouple Development and Instrumented EED Characteristics." Denver Research Institute, 31 March 1962.
3. Measurement Systems, Inc. "Quantum Detector for Measurement of EED Bridgewire Temperatures." 1 August 1962.
4. U. S. Naval Ordnance Test Station. "Selection and Operation of Infrared Detectors." 30 June 1961.
5. Cook, C. W. "The Sandia RF Testing Facility Using Low-Level Electromagnetic Radiation." Sandia Corp., Albuquerque, N. M., Proceedings of 2nd HERO Congress 1963, pp. 45-1 to 45-15.
6. Pollard, James R. "HERO Ground Plane Facility." USNWL, Technical Memo No. W-16/63 dated November 1963.
7. Miland, A. F., R. J. Colin, Jr. "An Aerospace Dilemma: The Incompatibility of Electromagnetics and Necessary Pyrotechnic Devices." Hughes Aircraft Company, Paper Presented at EMC Symposium, 1966, dated 6 July 1966.
8. Harrison, R. I., J. Zucher. "Hot-Carrier Microwave Detector." IEEE Proceedings, Vol. 54, No. 4, April 1966, pp. 588-595.
9. Kapsshilin, G. N. "Hot-Carrier Diode Opens New Vistas for Designers of High Frequency and Microwave Devices." hp Associates, Palo Alto, Calif., Electronic Design, 15 March 1966, pp. 178-185.
10. Parker, R. L. "A Low Level Electromagnetic Radiation Instrumentation System." Sandia Corp. Report No. 1424-2, dated 27 April 1961, pp. 41-59.

11. Wisseman, L. L. "A High Voltage Monolithic Operational Amplifier." Motorola Application Note AN-248, dated August 1966.
12. Widlar, R. J., J. N. Giles. "Designing with Off-the-Shelf Linear Microcircuits." Fairchild Application Bulletin APP-124, dated January 1966.
13. Chu, Yaohan. Digital Computer Design Fundamentals. McGraw-Hill Book Co., Inc., Copyright 1962, pp. 101-109.
14. Digital Logic Handbook - 1967. Digital Equipment Corporation, Maynard, Mass.
15. Tatro, R. D. "A Microcircuit Digital-to-Analog-Converter." Sprague Technical Paper TP-66-11 presented at the International Microelectronics Conference, Munich, Germany, October 1966.
16. hp Associates. "The Hot Carrier Diode Theory, Design, and Application." Application Note 907.

VITA

Jimmie Dick Burson

Candidate for the Degree of

Master of Science

Thesis: STATISTICAL STRAY ENERGY MONITOR

Major Field: Electrical Engineering

Biographical:

Personal Data: Born near McCurtain, Oklahoma, October 24, 1930, the son of Robert L. and Bertha T. Burson.

Education: Attended grade school in Hyde Park, Oklahoma; graduated from Central High School, Muskogee, Oklahoma in 1947; received the Associate of Arts degree from Muskogee Junior College in May 1957; received the Bachelor of Science degree from Oklahoma State University, with a major in Electrical Engineering, in May, 1959; completed requirements for the Master of Science degree in May, 1967.

Professional experience: Presently associated with North American Aviation, Inc. in the capacity of Project Engineer, Advanced Technology, responsible for the technical content and support of new business proposals. Has participated in various electronic and advanced systems design and proposal efforts on aerospace projects. Previously associated with the Research and Development Division of Collins Radio Co. working predominantly on the development of airborne weather radar utilizing solid-state devices. Registered as a Professional Engineer in the State of Oklahoma.